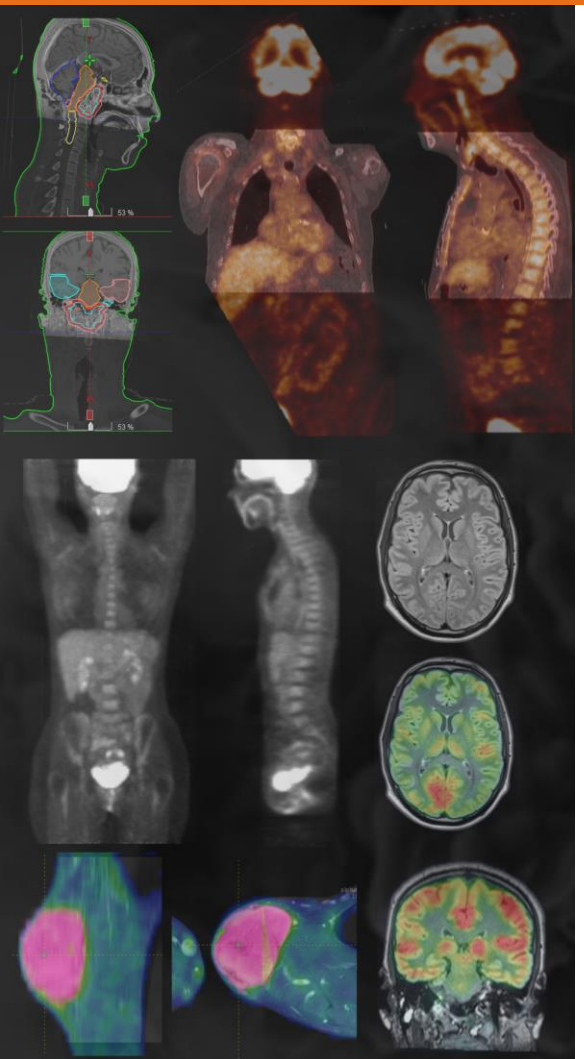

SNMMI 2025 - Bilan

- Cancer de la prostate – PSMA
- Cancer pulmonaire – *organomics*
- Radiopharmacie

09/07/2025

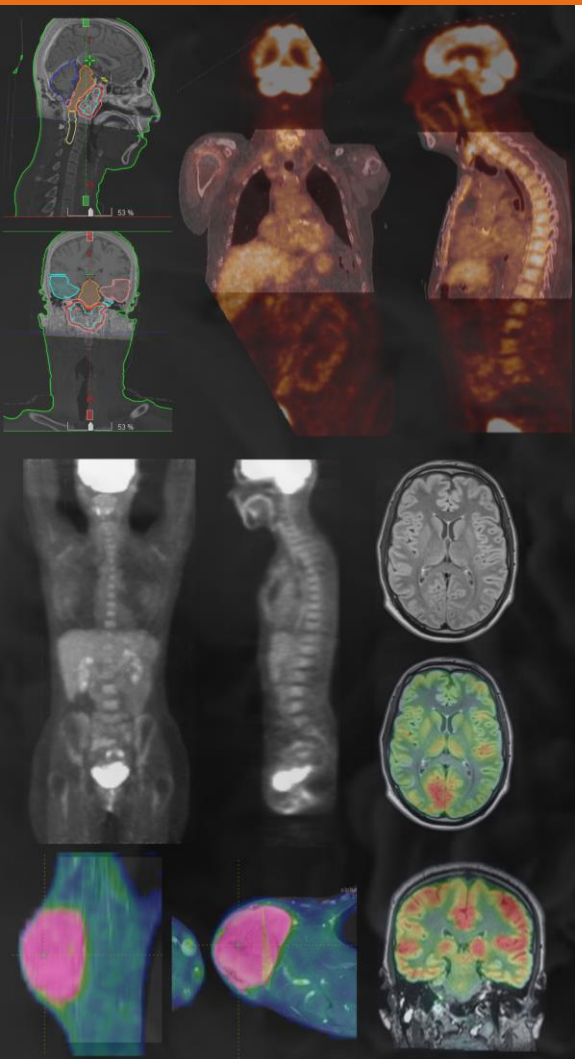

SNMMI 2025 - Bilan

- **Cancer de la prostate – PSMA**
- Cancer pulmonaire – *organomics*
- Radiopharmacie

09/07/2025

IOWA HEALTH CARE
University of Iowa Health Care

Are Bone Scans still necessary in the era of PSMA PET imaging?

Sanchay Jain MD, Michael M Graham PhD MD
Division of Nuclear Medicine, Radiology, University of Iowa Health Care, Iowa City, IA, United States

#251668

The University of Iowa

Methods

- Single-center retrospective study
- Included all patients between 2018-24:
  - With both a Tc^{99m} HDP bone scan and PSMA PET-CT imaging (either F^{18}-DCFPyL or Ga^{68}-PSMA)
  - **Within 60 days** of each other
  - Multiple imaging sets: Only one (first) pair included
- Comparison to identify additional and/or discordant (positive) bone scan findings which was otherwise negative (non-avid) on PSMA PET
- Patient chart reviewed by both authors to assess:
  - If these additional bone scan findings
    - Led to further diagnostic workup ?
    - Change in management ?
  - Changes on follow-up imaging in case of discordant lesions

Purpose	Methods	Results	Directions
Do bone scans provide additional information when performed in combination with PSMA PET-CT ?	➢ Retrospectively identified patients who underwent ▪ Bone scan AND PSMA PET-CT ▪ Within 60 days of each other ➢ Comparison of imaging findings ➢ Additional or discordant findings identified on bone scan: ▪ Review of imaging by both authors ▪ Chart review & review of follow-up imaging, if available	➢ 111 patients identified ➢ Only 7 patients with discordant/additional sites of uptake on bone scan ▪ 1 : Falsely negative PSMA PET and & changed management ▪ 1 : Multiple metastases on both scans; did not change management ▪ 5 : Likely false positive/benign variants; no change in management	✓ Bone scans provide minimal additional benefit when used together with PSMA PET-CT ✓ Simplification of PCa work-up ✓ Cost reduction

Implications

- Simplified work-up of Prostate Cancer
- Reduction in expenses
- May lead to a change in response assessment guidelines

Conclusion

- Bone scans provide minimal additional benefit when used in conjunction with PSMA PET-CT imaging in prostate cancer to identify additional sites of disease and effect treatment change
- In pre-treatment planning for Lu^{177}-PSMA therapy, the percentage of PSMA negative disease identified by bone scans is small and of questionable significance

Evaluating the PRIMARY Score: A Comparative Analysis of PSMA PET and mpMRI for Detecting Clinically Significant Prostate Cancer

Moein Moradpour[1], Lana Al Doori[2], Mona-Elisabeth R Revheim[3], Thomas Werner[1], Abass Alavi[1]

[1]University of Pennsylvania, Department of Radiology, Philadelphia, PA; [2]Drexel University College of Medicine, [3]Oslo University Hospital and University of Oslo

Purpose

- Multiparametric MRI (mpMRI) is the current standard for imaging in prostate cancer diagnosis but has limitations in negative or indeterminate cases, often leading to unnecessary biopsies.
- The 68Ga-PSMA-11 PET/CT-based PRIMARY score is a novel imaging tool that may offer enhanced diagnostic performance for clinically significant prostate cancer (csPCa).
- This study reviews the diagnostic value of the PRIMARY score, comparing it with mpMRI and evaluating its potential role in combined imaging strategies.

Methods

- Systematic literature review conducted using PubMed and Google Scholar
- Search terms included: *"PSMA PET," "Prostate Cancer," "PRIMARY score"*
- Extracted data on sensitivity, specificity, PPV, and NPV for PRIMARY score and mpMRI in detecting csPCa

Evaluating the PRIMARY Score: A Comparative Analysis of PSMA PET and mpMRI for Detecting Clinically Significant Prostate Cancer

Moein Moradpour[1], Lana Al Doori[2], Mona-Elisabeth R Revheim[3], Thomas Werner[1], Abass Alavi[1]

[1]University of Pennsylvania, Department of Radiology, Philadelphia, PA; [2]Drexel University College of Medicine, [3]Oslo University Hospital and University of Oslo

Results

Figure 1. Five-point PRIMARY score.

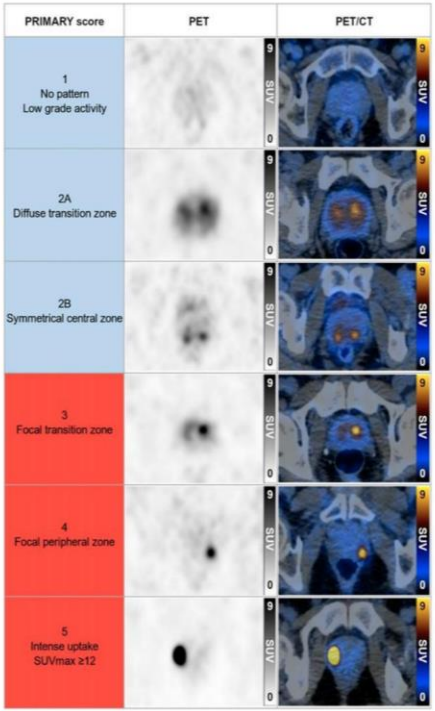

Diagnostic Performance of PRIMARY Score, mpMRI, and Combined Imaging in a 227-Patient Study

Modality	Sensitivity	Specificity	PPV	NPV
PRIMARY Score	86%	76%	88%	72%
mpMRI (PI-RADS)	89%	74%	88%	76%
Combined Imaging	94%	68%	86%	85%

Table 1: This table compares the diagnostic accuracy of PSMA PET using the PRIMARY score, mpMRI (PI-RADS), and a combination of both modalities in detecting clinically significant prostate cancer (csPCa). Combined imaging showed the highest sensitivity (94%) and negative predictive value (85%), suggesting improved performance when both techniques are used together.

PRIMARY Score vs. PI-RADS in a Multicenter Study of 291 Men

Modality	Sensitivity	Specificity	PPV	NPV
PRIMARY Score (1–2 vs. 3–5)	88%	64%	76%	81%
PI-RADS (Score 2 vs. 3–5)	83%	53%	69%	72%

Table 2. This figure illustrates the sensitivity, specificity, positive predictive value (PPV), and negative predictive value (NPV) of the PRIMARY score and PI-RADS in a multicenter cohort. The PRIMARY score outperformed PI-RADS in all categories, particularly in NPV (81% vs. 72%) and specificity (64% vs. 53%), indicating better ability to rule out csPCa.

Comparison of PRIMARY Score and PI-RADS in a 431-Patient Study

Modality	Sensitivity	Specificity	PPV	NPV
PRIMARY Score	90.6%	61.1%	71.4%	85.8%
PI-RADS	87.9%	49.0%	64.9%	79.1%

Table 3. This table presents performance metrics of the PRIMARY score and PI-RADS in a large patient cohort. The PRIMARY score showed higher sensitivity (90.6% vs. 87.9%), specificity (61.1% vs. 49.0%), PPV (71.4% vs. 64.9%), and NPV (85.8% vs. 79.1%), demonstrating superior diagnostic accuracy for detecting clinically significant prostate cancer.

Conclusion

- The PRIMARY score demonstrates strong diagnostic accuracy, with sensitivity and predictive performance comparable to—and in some cases better than—mpMRI.
- Combined use of PRIMARY and mpMRI improves diagnostic precision and may reduce unnecessary biopsies, particularly in patients with equivocal MRI findings.
- The PRIMARY score is a promising adjunct tool in prostate cancer imaging and may be applicable beyond 68Ga tracers with further research.
- Further studies are warranted to validate the PRIMARY score's performance with other PSMA PET tracers (e.g., 18F-labeled agents) and in broader clinical contexts.

#251888: Impact of ^{68}Ga-PSMA-11 PET/CT on Clinical Management of Prostate Cancer Patients in Different Clinical Settings

*Alireza Ghodsi, Avanti Gulhane, Ridvan Demirci, Jonathan Shuhendler, Roman Gulati, Atreya Dash, William Ellis, Yaw Nyame, George Schade, Jonathan Wright, Smith Apisarnthanarax, Jonathan Chen, Jay Liao, Kent Wallner, Heather Cheng, Petros Grivas, Andrew Hsieh, John Lee, Bruce Montgomery, Peter Nelson, Michael T. Schweizer, Todd Yezefski, John Wu, Rafee Talukder, Evan Y. Yu, Daniel W. Lin, Amir Iravani, **Delphine L. Chen***

2025 SNMMI Poster Award Candidate
2025 SNMMI Annual Meeting

Background

- Gallium-68 prostate-specific membrane antigen-11 positron emission tomography/computed tomography (^{68}Ga-PSMA-11 PET/CT) outperforms conventional imaging for detecting prostate cancer (PCa).
- There is limited data descriging how this advanced imaging influences clinical decisions in real-world clinical settings.

Purpose

- Investigating the impact of ^{68}Ga-PSMA-11 PET/CT on management at initial staging (IS), biochemical recurrence (BCR), and at either time point among patients with equivocal lesions on conventional imaging (EL).
- Examining the associations between scan positivity and PSMA-expressing total tumor volume (TTV) with baseline characteristics

Methods

- Patients with pathology-proven PCa were recruited into three cohorts:
  1. **IS** prior to planned definitive therapy for patients with Grade Group ≥4 disease or PSA >20.
  2. **BCR** (as defined by AUA or ASTRO) after surgery or radiation.
  3. **EL** based on conventional imaging obtained for IS (any grade disease) or BCR (any rise in PSA).
- Initial management plans were documented before ^{68}Ga-PSMA-11 PET/CT, and changes in management were tracked for up to 6 months after the scan and categorized as:
  - **Major:** change in treatment modality
  - **Minor:** modification within the same modality
- Multivariate models evaluated associations between scan positivity and TTV with clinical parameters, including age, Gleason score, PSA, and PSA doubling time (PSADT).
- IS and BCR cohorts included EL patients for multivariate analyses.

#251888: Impact of ^{68}Ga-PSMA-11 PET/CT on Clinical Management of Prostate Cancer Patients in Different Clinical Settings

Alireza Ghodsi, Avanti Gulhane, Ridvan Demirci, Jonathan Shuhendler, Roman Gulati, Atreya Dash, William Ellis, Yaw Nyame, George Schade, Jonathan Wright, Smith Apisarnthanarax, Jonathan Chen, Jay Liao, Kent Wallner, Heather Cheng, Petros Grivas, Andrew Hsieh, John Lee, Bruce Montgomery, Peter Nelson, Michael T. Schweizer, Todd Yezefski, John Wu, Rafee Talukder, Evan Y. Yu, Daniel W. Lin, Amir Iravani, ***Delphine L. Chen***

2025 SNMMI Poster Award Candidate

Results

101 men with a median age of 68 years (IQR: 64-74) were enrolled:

Characteristic		IS (N=29)	BCR (N=30)	EL (N=42)
Age		67 (62, 70)	71 (65, 75)	68 (65, 74)
PSA		16 (8, 31)	1 (1, 4)	9 (5,20)
WHO grade group		4 (3,5)	3 (2, 5)	3 (2, 5)
Gleason score	≤ 6	0 (0)	2 (6.7)	1 (2.4)
	7	10 (34)	17 (57)	21 (50)
	≥ 8	19 (66)	11 (37)	20 (48)

Changes in clinical management following ^{68}Ga-PSMA-11 PET/CT:

- **IS:** Management changed in **31%** of patients (8 major, 1 minor)
- **BCR:** Management changed in **60%** of patients (15 major, 3 minor)
- **EL:** Management changed in **62%** of patients (23 major, 3 minor)

Initial staging

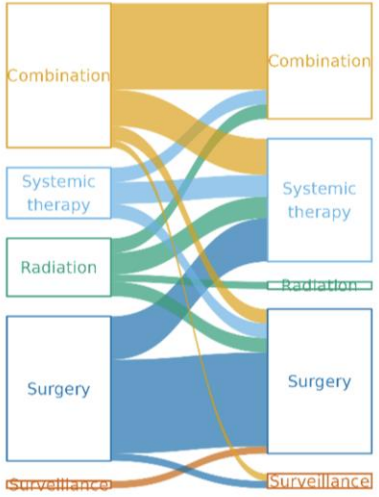

Biochemical recurrence

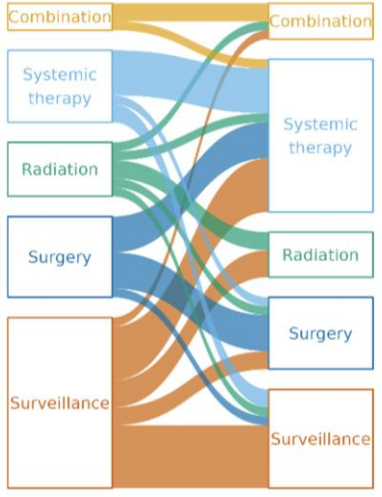

Equivocal lesions

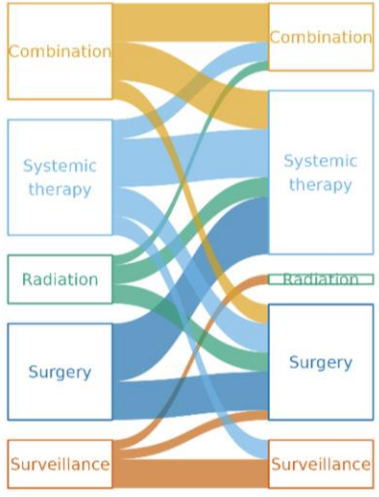

*Combination = use of at least two different treatment modalities

#251888: Impact of ^{68}Ga-PSMA-11 PET/CT on Clinical Management of Prostate Cancer Patients in Different Clinical Settings

Alireza Ghodsi, Avanti Gulhane, Ridvan Demirci, Jonathan Shuhendler, Roman Gulati, Atreya Dash, William Ellis, Yaw Nyame, George Schade, Jonathan Wright, Smith Apisarnthanarax, Jonathan Chen, Jay Liao, Kent Wallner, Heather Cheng, Petros Grivas, Andrew Hsieh, John Lee, Bruce Montgomery, Peter Nelson, Michael T. Schweizer, Todd Yezefski, John Wu, Rafee Talukder, Evan Y. Yu, Daniel W. Lin, Amir Iravani, ***Delphine L. Chen***

2025 SNMMI Poster Award Candidate
2025 SNMMI Annual Meeting

PSA was weakly associated with TTV after adjusting for age and Gleason score in the IS cohort (doubling PSA was associated with 1.3-fold increase in TTV; p=0.07) and strongly associated in the BCR cohort (1.6-fold increase; **p<0.001**) and EL cohort (1.5-fold increase; **p<0.001**).

Age and Gleason score were independently associated with TTV only in the **BCR cohort**.

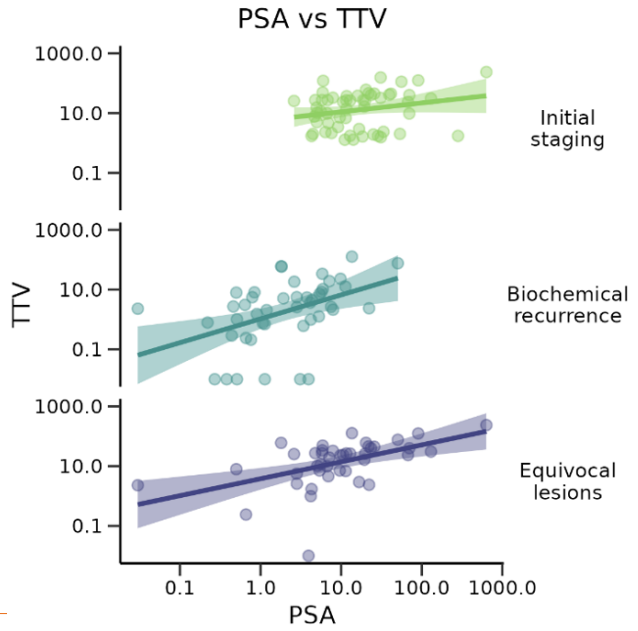

Conclusion

- ^{68}Ga-PSMA-11 PET/CT is a promising diagnostic method for patients with PCa in clinical practice, achieving a **94%** overall detection rate.
- It impacted clinical management in **58%** of cases, especially in patients with **BCR or equivocal lesions**.

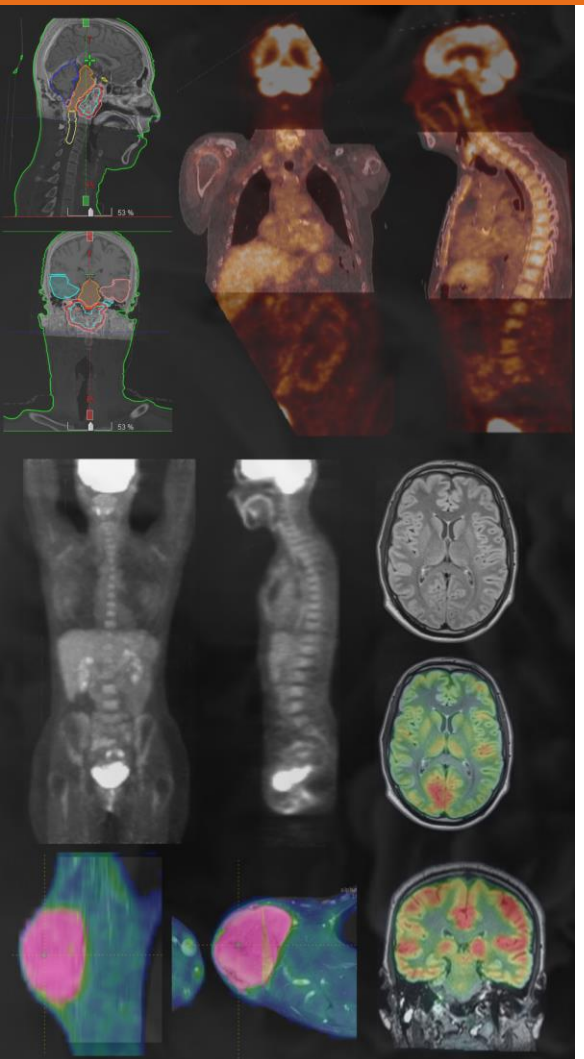

SNMMI 2025 - Bilan

- Cancer de la prostate – PSMA
- **Cancer pulmonaire – *organomics***
- Radiopharmacie

09/07/2025

Knowledge-based semantic enrichment of medical imaging data for automatic phenotyping and pattern discovery in metastatic lung cancer

Francesco Cremonesi[1], Lucie Chambon[1], Nelson Mokaddem[2], Huyen Trang Nguyen[1], Olivier Humbert[2,3], Marco Lorenzi[1]
[1] Inria Center at Université Côte d'Azur, Epione Research Group, France
[2] Department of Nuclear Medicine, Centre Antoine Lacassagne, Université Côte d'Azur (UCA), 33 Avenue de Valombrose, 06189 Nice, France
[3] Université Côte d'Azur, CNRS, Inserm, iBV, Nice, France

1. INTRODUCTION

A) CONTEXT

The emergence of AI models for the segmentation of 18-FDG PET/CT images has opened the way for **automatic quantification of clinically-relevant parameters in metastatic cancer patients**. However, current approaches **lack specificity** as they do not provide information about the localisation of lesions, which is a major clinical parameter for patient management. These methods also **lack generality**, as they fail to integrate the medical community's body of anatomical knowledge, which can nowadays be found in machine-readable ontology formats.

B) OBJECTIVES

Semantic enrichment of lesion annotations through the automatic segmentation of anatomical structures and inclusion of ontological knowledge. Demonstrate how such integration improves analysis depth, interpretability, as well as reusability of the data for secondary purposes, by enabling reasoning at different anatomical scales and linking with other sources of information such as clinical records.

C) DATA

Whole-body 18-FDG PET/CT scans from a cohort of **metastatic non-small cell lung cancer (NSCLC) patients undergoing immunotherapy treatment** (*n=101*) from Centre Antoine Lacassagne were included. The dataset included:
i) **automatic organ segmentations on CT** using TotalSegmentator [1]
ii) **manual lesion segmentations on FDG PET** by doctors
iii) **Manual annotation of lesion location** ,at the organ level, by doctors, termed « **reference organ labels of lesions** »

[1] Wasserthal, Jakob, et al. "TotalSegmentator: robust segmentation of 104 anatomic structures in CT images." *Radiology: Artificial Intelligence* 5.5 (2023): e230024.
[2] Rosse, Cornelius, and José LV Mejino Jr. "A reference ontology for biomedical informatics: the Foundational Model of Anatomy." Journal of biomedical informatics 36.6 (2003): 478-500.

Knowledge-based semantic enrichment of medical imaging data for automatic phenotyping and pattern discovery in metastatic lung cancer

Francesco Cremonesi[1], Lucie Chambon[1], Nelson Mokaddem[2], Huyen Trang Nguyen[1], Olivier Humbert[2,3], Marco Lorenzi[1]
[1] Inria Center at Université Côte d'Azur, Epione Research Group, France
[2] Department of Nuclear Medicine, Centre Antoine Lacassagne, Université Côte d'Azur (UCA), 33 Avenue de Valombrose, 06189 Nice, France
[3] Université Côte d'Azur, CNRS, Inserm, iBV, Nice, France

2. METHODS

A) MAPPING IMAGING STRUCTURES TO ANATOMICAL KNOWLEDGE

We mapped the roughly 100 TotalSegmentator structures and the human-defined gold-standard labels to the Foundational Model of Anatomy (FMA) ontology [2] using a mix of automatic heuristics and human post-hoc oversight. Each structure was then associated with **reference organ labels of lesions** by querying the ontology using the SparQL language for hierarchical or inclusion relationships such as *subClassOf*, *member_of*, and others. A small number of associations between one anatomical structure and multiple gold-standard labels were refined using simple prioritization heuristics.

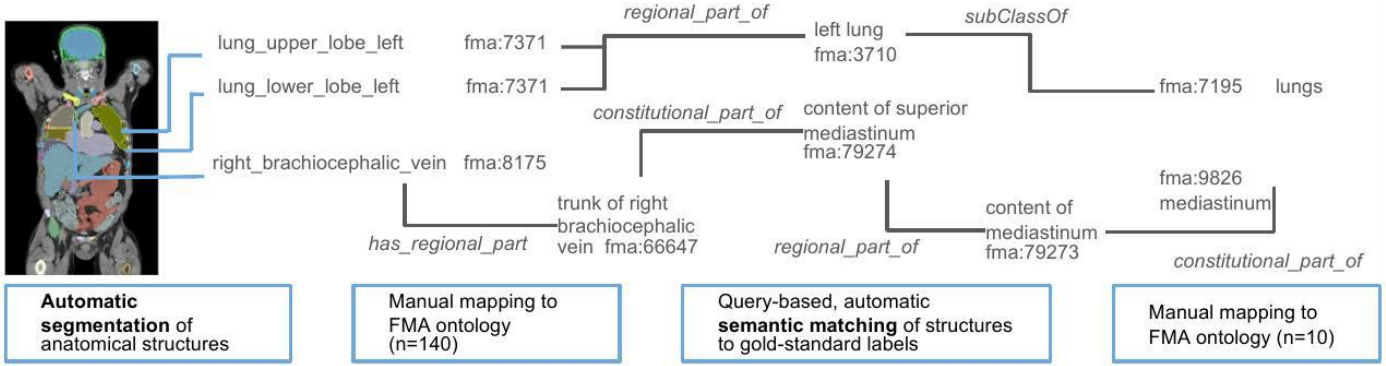

Knowledge-based semantic enrichment of medical imaging data for automatic phenotyping and pattern discovery in metastatic lung cancer

Francesco Cremonesi[1], Lucie Chambon[1], Nelson Mokaddem[2], Huyen Trang Nguyen[1], Olivier Humbert[2,3], Marco Lorenzi[1]
[1] Inria Center at Université Côte d'Azur, Epione Research Group, France
[2] Department of Nuclear Medicine, Centre Antoine Lacassagne, Université Côte d'Azur (UCA), 33 Avenue de Valombrose, 06189 Nice, France
[3] Université Côte d'Azur, CNRS, Inserm, iBV, Nice, France

B) KNOWLEDGE-ENHANCED IMAGING DATABASE

We computed the intersection between the manual lesion segmentations on PET performed by doctors and the automatic organ segmentations on CT, generated by TotalSegmentator, and combined intersections belonging to the same class as defined by the **reference organ labels of lesions**. We localised lesions by finding classes with the maximal intersection.

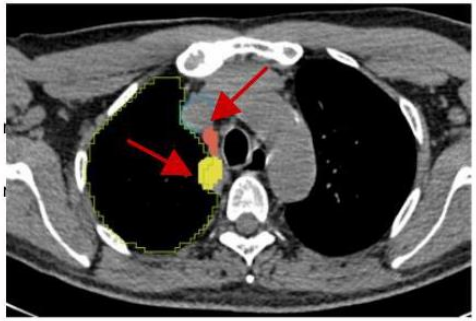

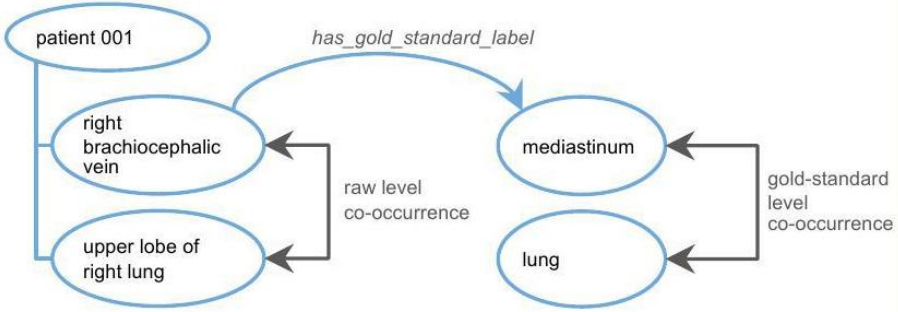

A Knowledge Graph (KG) integrating the FMA ontology allows the extraction of the co-occurrence of lesions at two semantic scales: the raw TotalSegmentator structures and the **reference organ labels**. In both cases, we perform KMeans clustering to stratify patients based on patterns of lesion co-occurrence.

Knowledge-based semantic enrichment of medical imaging data for automatic phenotyping and pattern discovery in metastatic lung cancer

Francesco Cremonesi[1], Lucie Chambon[1], Nelson Mokaddem[2], Huyen Trang Nguyen[1], Olivier Humbert[2,3], Marco Lorenzi[1]
[1] Inria Center at Université Côte d'Azur, Epione Research Group, France
[2] Department of Nuclear Medicine, Centre Antoine Lacassagne, Université Côte d'Azur (UCA), 33 Avenue de Valombrose, 06189 Nice, France
[3] Université Côte d'Azur, CNRS, Inserm, iBV, Nice, France

Knowledge-based semantic enrichment of medical imaging data for automatic phenotyping and pattern discovery in metastatic lung cancer

Francesco Cremonesi[1], Lucie Chambon[1], Nelson Mokaddem[2], Huyen Trang Nguyen[1], Olivier Humbert[2,3], Marco Lorenzi[1]
[1] Inria Center at Université Côte d'Azur, Epione Research Group, France
[2] Department of Nuclear Medicine, Centre Antoine Lacassagne, Université Côte d'Azur (UCA), 33 Avenue de Valombrose, 06189 Nice, France
[3] Université Côte d'Azur, CNRS, Inserm, iBV, Nice, France

3. RESULTS

Ontology-based mapping of anatomical structures enabled automatic validation of the lesion localization algorithm. The simple intersection-based algorithm **successfully localized 1572 out of 1962 lesions (80.1 %)** across all lesion sizes.

Patient phenotyping based on the knowledge-enhanced organ labels allowed for **more interpretable clusters** that could be used for **better correlation with survival metrics** and more precise quantitative imaging

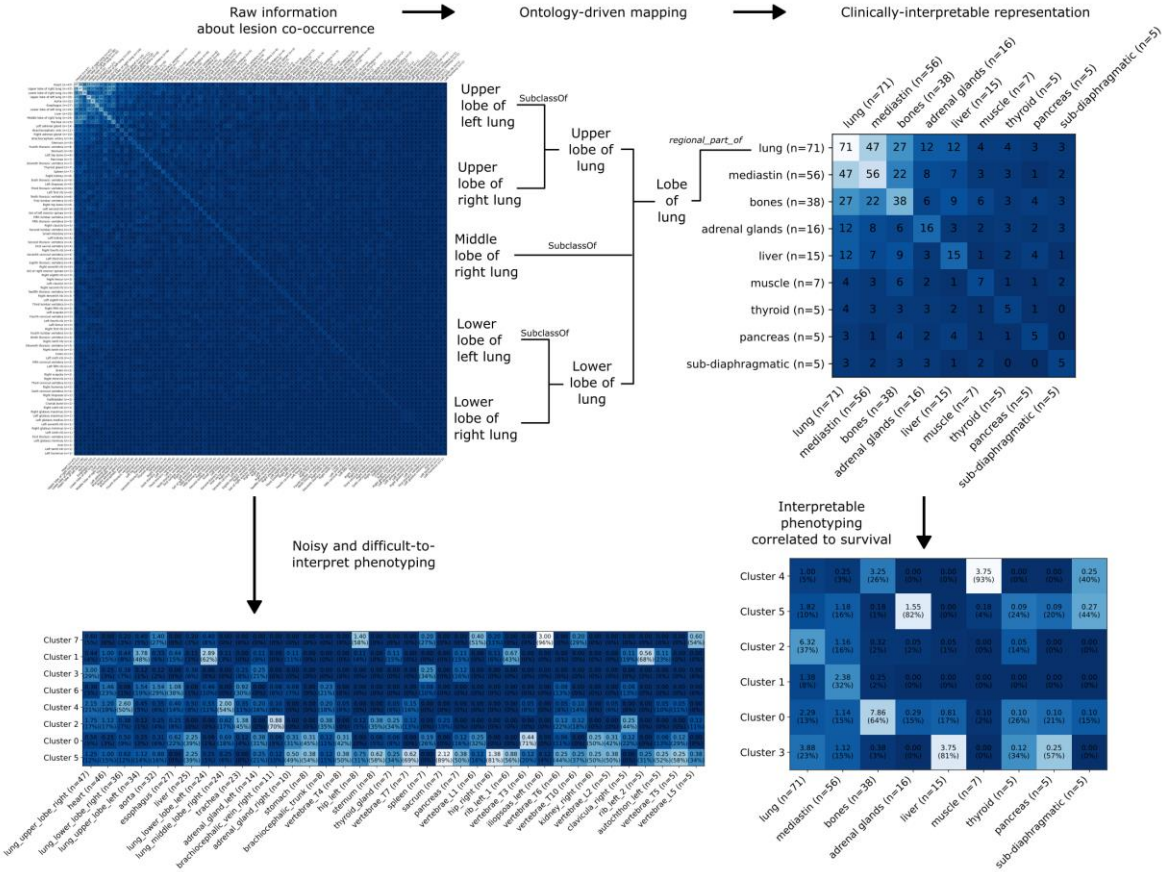

MetaPredictomics: A Comprehensive Approach to Predict Post-Surgical NSCLC Recurrence Using Clinicopathological, Radiomics, and Organomics Data

Mehdi Amini[1], Ghasem Hajianfar[1], Yazdan Salimi[1], Zahra Mansouri[1], and Habib Zaidi[1†]

[1]Division of Nuclear Medicine and Molecular Imaging, Geneva University Hospital, Geneva, Switzerland

This work was supported by the Swiss National Science Foundation with grant SNRF 320030_231742

METHODS

- Dataset: 145 NSCLC patients sourced from an online dataset.
- Segmentation: A fully automated deep learning model to delineate 19 organs on the CT compartment of the pre-surgical PET/CT scans.
- Radiomics: Using PyRadiomics, 214 features (107 from CT, 107 from PET) were extracted from the gross tumor volume (GTV) and each segmented organ.
- Clinical feature set: based on clinicopathological, gene mutation status, and treatment history.

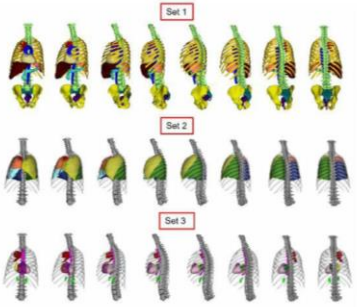

Figure 1. An example of the organs segmented on the CT image of a patient in 3D visualization.

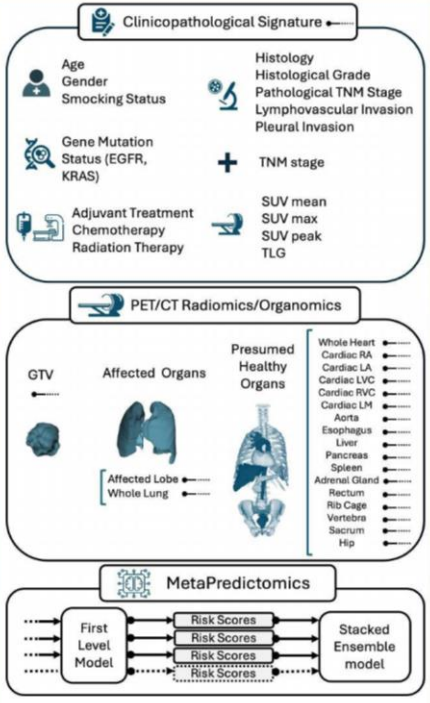

Figure 2. The proposed MetaPredictomics framework for predicting NSCLC recurrence.

- First level model: a time-to-event prediction machine, based on Glmboost.
- Meta Model: The hazard ratios obtained from the first level models were then used as inputs for meta models developed using a stacked ensemble approach.
- Questing optimized performance, we assessed meta models established upon all possible combinations of first level models with C-index≥0.6.
- Evaluation: The performance of all the models was evaluated using the average concordance index (C-index) across a unique 3-fold cross validation scheme for fair comparison.

MetaPredictomics: A Comprehensive Approach to Predict Post-Surgical NSCLC Recurrence Using Clinicopathological, Radiomics, and Organomics Data

Mehdi Amini[1], Ghasem Hajianfar[1], Yazdan Salimi[1], Zahra Mansouri[1], and Habib Zaidi[1†]

[1]Division of Nuclear Medicine and Molecular Imaging, Geneva University Hospital, Geneva, Switzerland

This work was supported by the Swiss National Science Foundation with grant SNRF 320030_231742

RESULTS

- The Clinicopathological model outperformed other first level models with C-index of 0.67.
- GTV radiomics model achieved C-index of 0.65.
- Among the organomics models, whole-lung and aorta models achieved top performance with C-index of 0.65.
- In total 12 organomics models achieved C-indices of ≥ 0.6.

Table 1. The results of the first-level models for each test fold as well as the average value of the three test folds in concordance index (C-index).

Model	Fold 1	Fold 2	Fold3	Average
Clinicopathological	0.74	0.69	0.57	0.67
GTV	0.71	0.62	0.61	0.65
Affected Lung Lobe	0.66	0.63	0.59	0.63
Whole Lung	0.72	0.63	0.61	0.65
Whole Heart	0.61	0.6	0.6	0.6
Cardiac Right Artrium	0.58	0.56	0.59	0.58
Cardiac Left Artium	0.58	0.55	0.6	0.58
Cardiac Left Ventricle Cavity	0.65	0.57	0.59	0.61
Cardiac Right Ventricle Cavity	0.6	0.6	0.6	0.6
Cardiac Left Myocardium	0.59	0.57	0.61	0.59
Aorta	0.67	0.58	0.68	0.65
Esophagus	0.62	0.65	0.63	0.63
Liver	0.67	0.58	0.59	0.62
Pancreas	0.58	0.62	0.62	0.61
Spleen	0.59	0.61	0.59	0.6
Adrenal Glands	0.62	0.57	0.69	0.63
Rectum	0.57	0.56	0.6	0.58
Rib Cage	0.61	0.56	0.6	0.59
Vertebra	0.58	0.56	0.62	0.59
Sacrum	0.62	0.6	0.62	0.62
Hip	0.56	0.57	0.59	0.58

- Meta models significantly outperformed the first level models with the top 100 achieving C-indices between 0.703 to 0.731.
- The clinicopathological, whole lung, esophagus, pancreas, and GTV models were the most frequently present models in the top 100 meta models with frequencies of 98, 71, 69, 62, 61, respectively.

Table 2. The performance of the top 10 meta-models sorted by their average C-index over the three test folds. Result of each fold is as well presented.

	Models	Fold 1	Fold 2	Fold 3	Average
1	Clinical+GTV+Whole Lung+Esophagus+Pancreas	0.800	0.685	0.709	0.731
2	Clinical+GTV+Whole Lung+Sacrum	0.816	0.639	0.738	0.731
3	Clinical+GTV+Whole Lung+Pancreas+Sacrum	0.816	0.641	0.731	0.730
4	Clinical+Affected Lung Lobe+Whole Lung+Esophagus+Pancreas	0.766	0.725	0.696	0.729
5	Clinical+Whole Lung+Esophagus	0.783	0.733	0.670	0.729

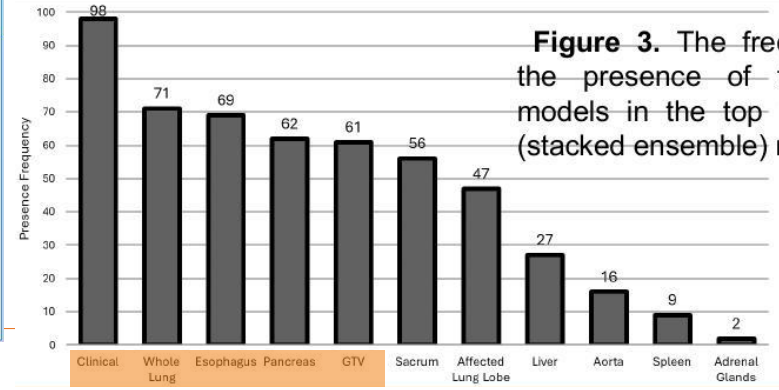

Figure 3. The frequency of the presence of first level models in the top 100 meta (stacked ensemble) models.

CONCLUSION

In this study we highlighted the value of maximizing the use of medical imaging for NSCLC recurrence prognostication by incorporating data from various organs, rather than focusing solely on the tumor and its immediate surroundings.

This multi-source integration proved particularly beneficial in the meta models, where combining clinicopathological data with tumor radiomics and organomics models significantly enhanced recurrence prediction.

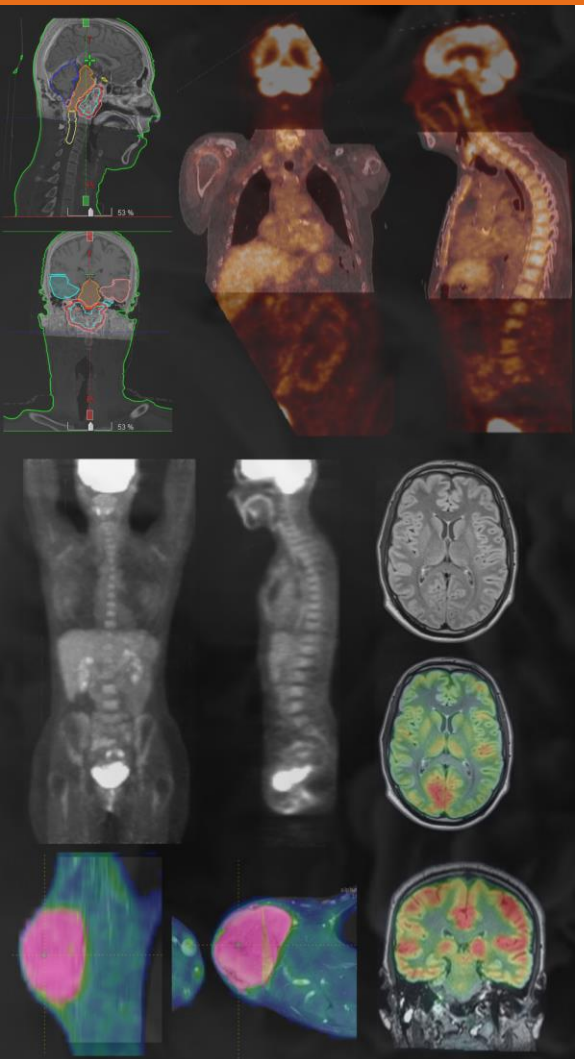

SNMMI 2025 - Bilan

- Cancer de la prostate – PSMA
- Cancer pulmonaire – *organomics*
- **Radiopharmacie**

09/07/2025

Assessment of PET Drug Adverse Events over the Last Half Century

Marianna Dakanali[1,2], Peter J. H. Scott[1,2], Henry F. VanBrocklin[2,3], Steven S. Zigler[2,4]

[1] Department of Radiology, University of Michigan, Ann Arbor, MI
[2] Coalition of PET Drug Manufacturers, Fredericksburg, TX
[3] Department of Radiology and Biomedical Imaging, University of California San Francisco, San Francisco, CA
[4] Siemens PETNET Solutions, Knoxville, TN

2025 SNMMI Poster Award Candidate

Introduction

Multiple new PET Radiopharmaceuticals (RPhs) have recently been approved by the US Food and Drug Administration (FDA). Despite the generally accepted safety profile of PET RPhs over millions of studies per year, the microdoses used in most studies, and low incidence of adverse events (AEs),[1-4] there appear to be elevated concerns from regulatory authorities regarding the safety of PET RPhs in recent years. The FDA Adverse Events Reporting System (FAERS) Public Dashboard was established in 1969 and is an open access database which collects AEs or other pharmaceutical errors reported by patients, providers or the drug manufacturers.[5] This retrospective study assesses risks associated with PET RPhs by reviewing AEs reported through FAERS since 21 CFR 212 was implemented in 2012.

Methods

Data for AEs reported to FDA for approved PET RPhs were collected using FAERS during December 2024 for global AEs reported between 2012 and September 30th, 2024. FDA approved PET radiopharmaceuticals were searched using all known names for each drug, both generic and brand names. The following tables were downloaded from the database: a. case count by received year; b. cases by reaction; and c. listing of cases. AE reports were categorized as depicted in **Figure 1**.

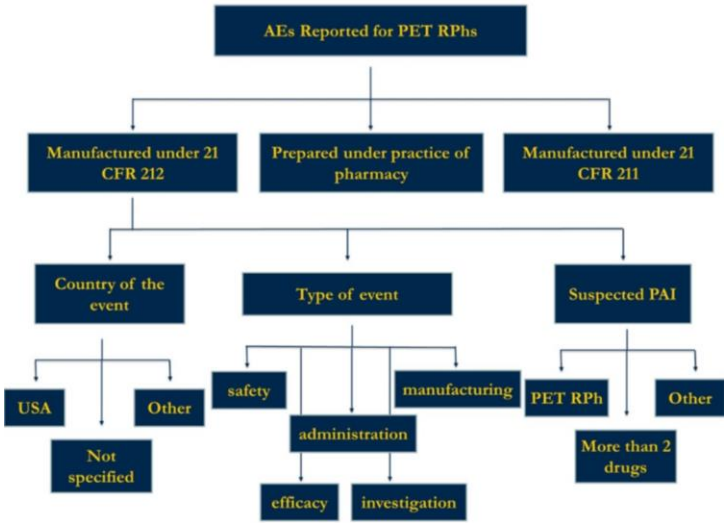

Figure 1. AEs were categorized based on manufacturing regulatory oversight. RPhs manufactured under 21 CFR 212 were further analyzed based on country of the event, type of the event and suspected Product Active Ingredient (PAI)

Assessment of PET Drug Adverse Events over the Last Half Century

Marianna Dakanali[1,2], Peter J. H. Scott[1,2], Henry F. VanBrocklin[2,3], Steven S. Zigler[2,4]

[1] Department of Radiology, University of Michigan, Ann Arbor, MI
[2] Coalition of PET Drug Manufacturers, Fredericksburg, TX
[3] Department of Radiology and Biomedical Imaging, University of California San Francisco, San Francisco, CA
[4] Siemens PETNET Solutions, Knoxville, TN

2025 SNMMI Poster Award Candidate

Results

Collectively, more than 23.2 million AE reports for all drug products were transmitted to FDA between January 2012 and September 2024. The total number of reports submitted for all FDA-approved PET RPhs was 1,011. Of those, 7 cases were removed as duplicates bringing the total number of reports to 1,004, representing only 0.0043% of AEs reported to the FDA for the specified time period. Of these 1,004

Reported AEs Based on Country Event Occurred

Of the 1,004 total cases, 810 (81%) occurred in the US, 133 (13%) in other countries, while the country for the remaining 61 cases (6%) was not specified (**Figure 3A**). For the 508 AEs associated with PET RPhs manufactured under the cGMP requirements in 21 CFR 212, only 353 of the reported AEs occurred in the United States (**Figure 3B**).

Reported AEs Based on Type of Event Reported

The 508 reported cases for PET RPhs manufactured according to 21 CFR 212 were classified based on the type of event reported. Events were categorized as related to safety or efficacy of the drug, drug administration errors, manufacturing problems, and events reported as either a false positive or false negative investigation. The results are depicted in **Figure 4** and detailed in **Table 1**.

21 CFR Part 212 – Current Good Manufacturing Practice for Positron Emission Tomography (PET) Drugs

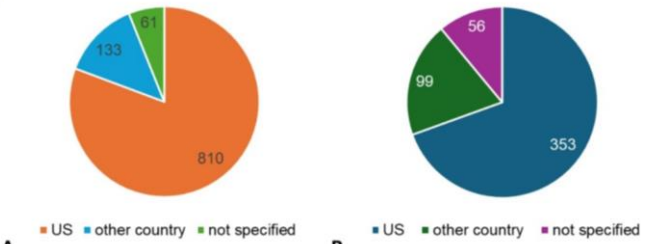

Figure 3: **A.** Number of reports for PET RPhs based on the country where the event urred. **B.** Number of reports for PET RPhs manufactured under 21 CFR part 212 ed on the country where the event occurred.

Table 1: Adverse Events Categorized by Type and Radiopharmaceutical

Drug	Safety	Efficacy	Administration	Investigation	Manufacturing
Ammonia N-13	2	0	0	0	0
Fluciclovine F-18	14	34	15	11	2
Fluoroestradiol F-18	1	1	0	4	0
Florbetaben F-18	6	0	0	0	0
Florbetapir F-18	55	2	6	0	1
Flutemetamol F-18	81	5	1	0	0
Sodium Fluoride F-18	1	1	0	0	0
Flotufolastat F-18	1	9	0	1	0
Piflufolastat F-18	24	60	9	3	19
Fludeoxyglucose F-18	115	7	6	1	10
Total	**300**	**119**	**37**	**20**	**32**

Conclusions

Despite the increased concerns regarding the safety of PET RPhs from regulators in recent years, our analysis of the AEs reported to the FAERS public dashboard revealed that the number of AEs remains extremely low (less than 81 AEs per 10^6 scans per year) compared to the annual number of doses administered (estimated at about 3,000,000).[6] These findings confirm our assertion that PET radiopharmaceuticals can be generally recognized as a safe and effective drug class, for which very low levels of adverse events are observed year to year. It is challenging to conclusively connect reported AEs to PET RPh sterility or production failures and thus, in our opinion this should not be used to justify any revision of regulations.

Prediction of blood-brain barrier penetration of PET CNS drugs enabled by explainable machine learning

Clemens P. Spielvogel[1], Natalie Schindler[1], Christian Schroeder[2], Sarah Stellnberger[3], Wolfgang Wadsak[1], Markus Mitterhauser[1], Laszlo Papp[4], Marcus Hacker[1], Verena Pichler[3], Chrysoula Varka[1]

MEDIZINISCHE UNIVERSITÄT WIEN

- Aim 1: To establish a public database of radiolabeled drug candidates and their ability to permeate the BBB
- Aim 2: To employ explainable machine learning to identify radiolabeled drug candidates capable of penetrating the blood-brain barrier (BBB)

propriétés physico-chimiques issues de **mesures expérimentales** et de **méthodes in silico**

- Data from **experimental and computed** sources
- Molecular weight, logP, H-bond donors/acceptors
- Classical PSA and **novel 3D PSA**
- **Established scores**: CNS MPO, BBB score, CNS MPO PET

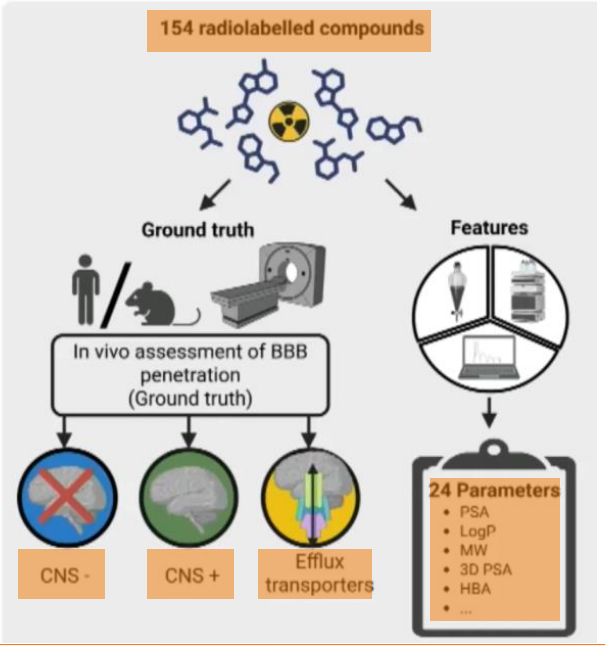

Prediction of blood-brain barrier penetration of PET CNS drugs enabled by explainable machine learning

Clemens P. Spielvogel[1], Natalie Schindler[1], Christian Schroeder[2], Sarah Stellnberger[3], Wolfgang Wadsak[1], Markus Mitterhauser[1], Laszlo Papp[4], Marcus Hacker[1], Verena Pichler[3], Chrysoula Varka[1]

MEDIZINISCHE UNIVERSITÄT WIEN

- **Binary classification** (CNS+ vs. CNS−)
- **Multi-class** (CNS+, CNS−, Efflux)

- Six ML algorithms
- **100× Monte Carlo cross-validation**
- Explainability: **SHAP + Surrogate Models**

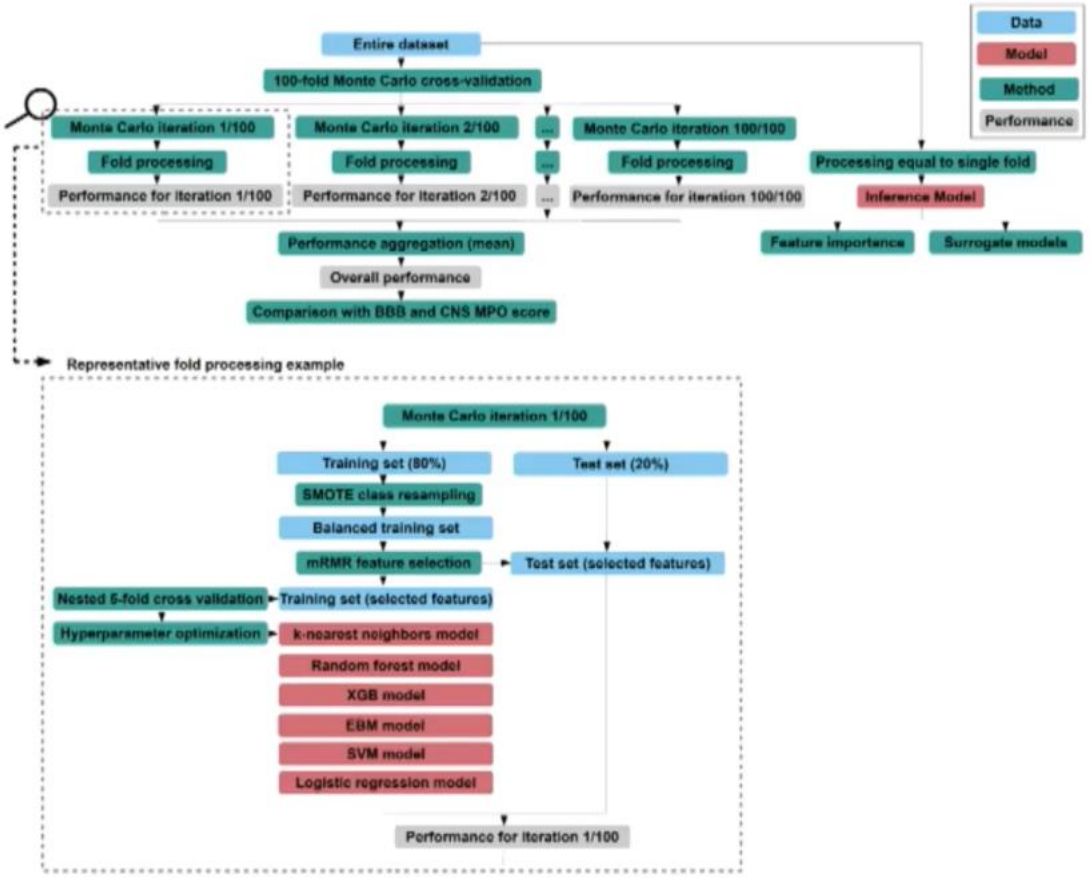

Prediction of blood-brain barrier penetration of PET CNS drugs enabled by explainable machine learning

Clemens P. Spielvogel[1], Natalie Schindler[1], Christian Schroeder[2], Sarah Stellnberger[3], Wolfgang Wadsak[1], Markus Mitterhauser[1], Laszlo Papp[4], Marcus Hacker[1], Verena Pichler[3], Chrysoula Varka[1]

MEDIZINISCHE UNIVERSITÄT WIEN

- **Random Forest – Best AUC:**
  - Binary: **AUC 0.88** (95% CI 0.87–0.90)
  - Multiclass: **AUC 0.82** (95% CI 0.81–0.82)
- Individual features weak predictors: AUC < 0.57
- **ML outperforms traditional scores**
  - CNS MPO (AUC 0.53), CNS MPO PET (AUC 0.51), BBB Score (AUC 0.68)

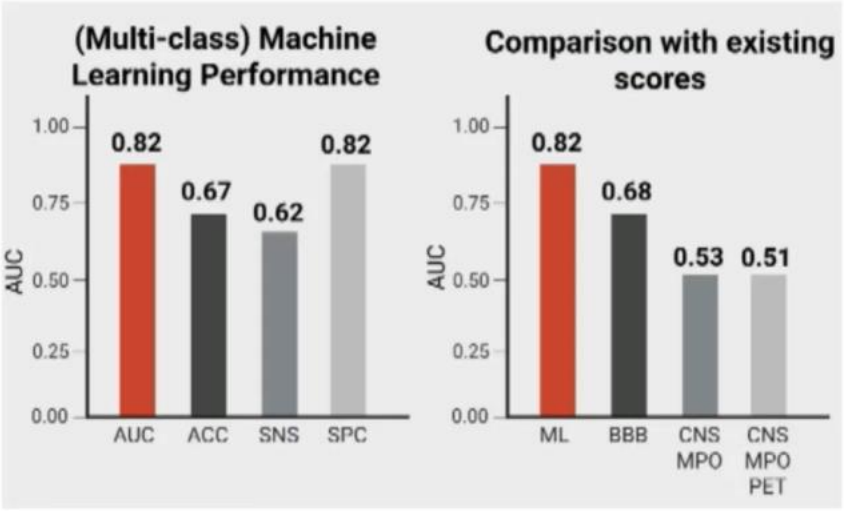

Prediction of blood-brain barrier penetration of PET CNS drugs enabled by explainable machine learning

Clemens P. Spielvogel[1], Natalie Schindler[1], Christian Schroeder[2], Sarah Stellnberger[3], Wolfgang Wadsak[1], Markus Mitterhauser[1], Laszlo Papp[4], Marcus Hacker[1], Verena Pichler[3], Chrysoula Varka[1]

MEDIZINISCHE UNIVERSITÄT WIEN

Binary classification (CNS -/+)

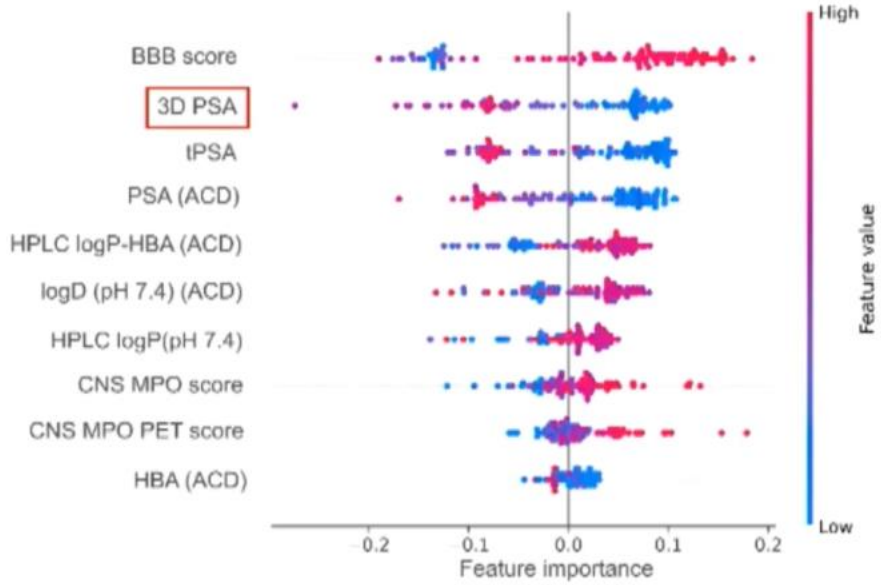

Multi-class classification (CNS -/+/efflux)

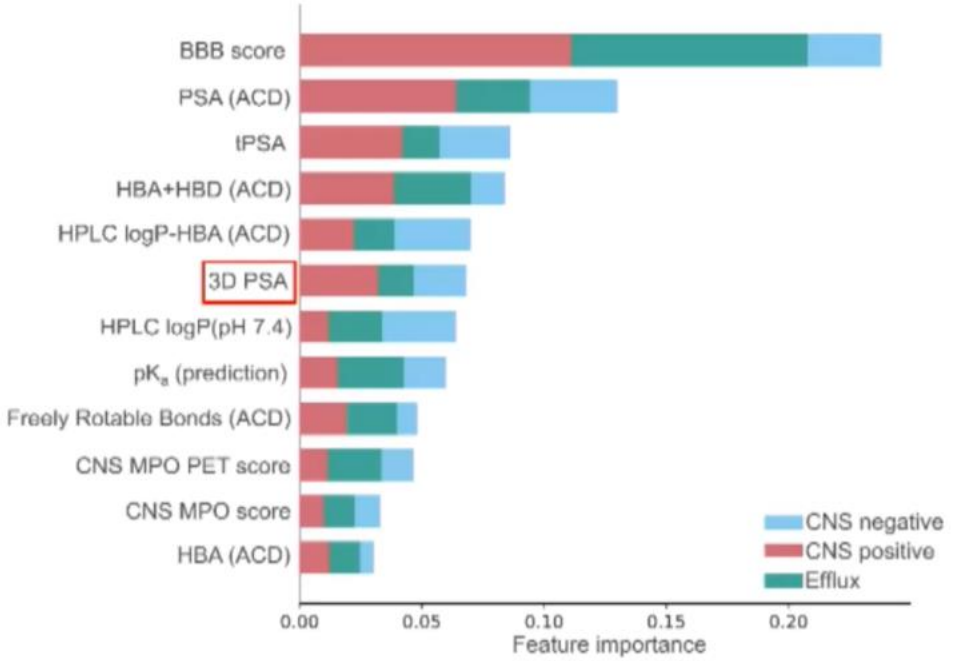

Prediction of blood-brain barrier penetration of PET CNS drugs enabled by explainable machine learning

Clemens P. Spielvogel[1], Natalie Schindler[1], Christian Schroeder[2], Sarah Stellnberger[3], Wolfgang Wadsak[1], Markus Mitterhauser[1], Laszlo Papp[4], Marcus Hacker[1], Verena Pichler[3], Chrysoula Varka[1]

MEDIZINISCHE UNIVERSITÄT WIEN

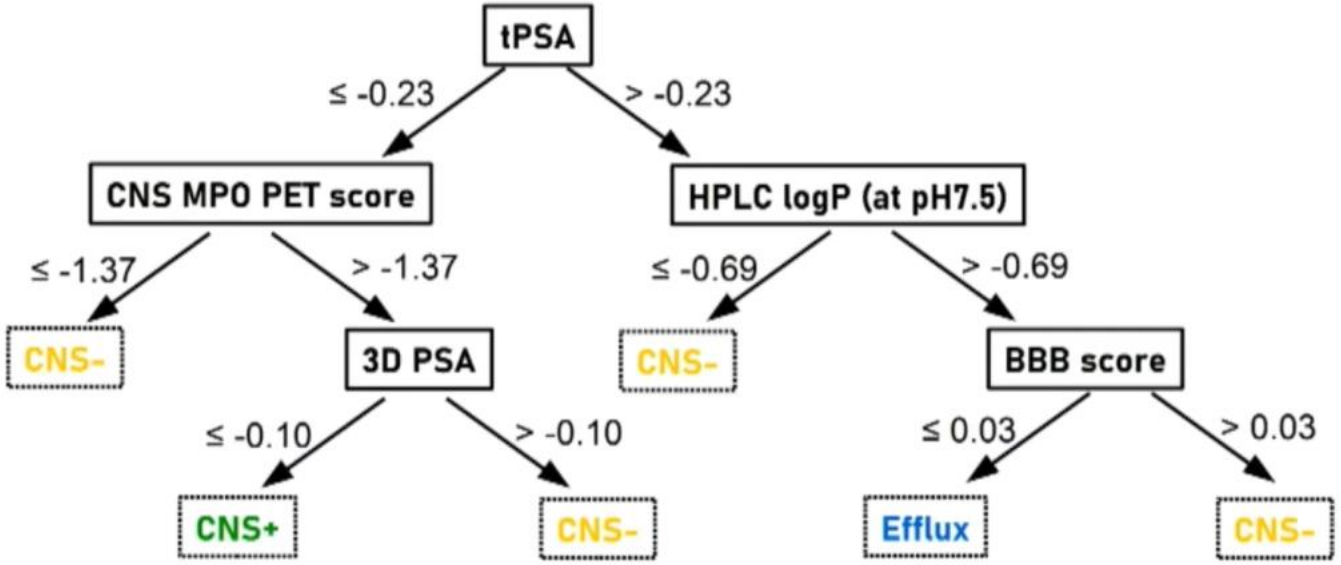

Are Bone Scans still necessary in the era of PSMA PET imaging?

Sanchay Jain MD, Michael M Graham PhD MD
Division of Nuclear Medicine, Radiology, University of Iowa Health Care, Iowa City, IA, United States

#251668

Background

- **Radionuclide bone imaging** (Tc^{99m}-labeled MDP/HDP) in evaluation of prostate cancer (PCa)
  - Traditional cornerstone in the metastatic workup
  - Commonly used prior to Lu^{177}-PSMA therapy
  - Often used NucMed modality to assess response in (radionuclide therapy) clinical trials
  - High false positive rate[1]
- Prostate-specific membrane antigen **(PSMA) PET** with agents such as Ga^{68}-PSMA or F^{18}-DCFPyL
  - Has become standard-of-care in PCa management
  - Receptor targeted; inherently more specific and identifies more lesions than bone scan[2]
- This study evaluated if bone scans:
  - Provide any **additional** diagnostic value
  - Influence clinical **management**
  - *when performed in **combination** with* PSMA PET

Methods

- Single-center retrospective study
- Included all patients between 2018-24:
  - With both a Tc^{99m} HDP bone scan and PSMA PET-CT imaging (either F^{18}-DCFPyL or Ga^{68}-PSMA)
  - **Within 60 days** of each other
  - Multiple imaging sets: Only one (first) pair included
- Comparison to identify additional and/or discordant (positive) bone scan findings which was otherwise negative (non-avid) on PSMA PET
- Patient chart reviewed by both authors to assess:
  - If these additional bone scan findings
    - Led to further diagnostic workup ?
    - Change in management ?
  - Changes on follow-up imaging in case of discordant lesions
- Study summary ▶

Representative cases

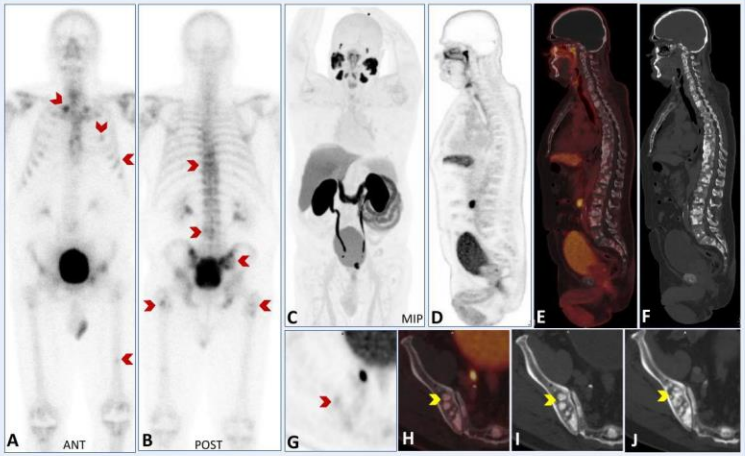

Fig 1: True Positive bone scan False Negative PSMA, probably because tumor was PSMA-negative. 73-year-old male with recently diagnosed PCa (Gleason 10, WHO GG5, PSA 16.2 ng/mL) underwent staging bone scan and a F^{18}-DCFPyL PET-CT. Baseline bone scan (A,B) showed multiple metastases (red arrows). Baseline PET-CT (C-I) showed no significant tracer uptake at the site of widespread sclerotic skeletal lesions. He was then started on Androgen deprivation therapy (ADT) and subsequently received Docetaxel. Follow-up CT at 6 months showed increase in extent of sclerotic lesions; progression in representative right iliac bone lesions (orange arrows in J), which made the differential of osteopoikilosis much less likely. At three years PSA is <0.03 ng/mL.

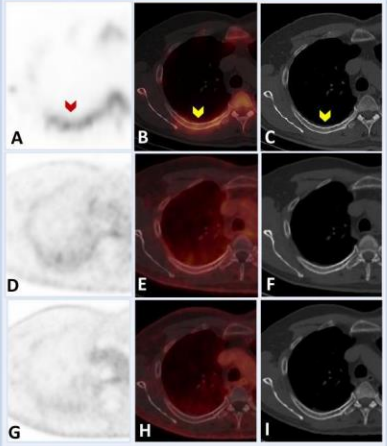

Fig 2: False Positive bone scan True Negative PSMA 65-year-old male with newly diagnosed PCa (Gleason 9, WHO GG5, PSA 7.56 ng/mL). Staging bone scan showed uptake in right 5th rib (arrows) on SPECT/SPECT-CT (A, B), but no CT changes (C). No uptake on baseline (D-F) & follow-up (G-I) Ga^{68} PSMA PET (6y interval) at this site. PSA was <0.03 ng/mL following prostatectomy.

Summary

Purpose	Methods	Results	Directions
Do bone scans provide additional information when performed in combination with PSMA PET-CT ?	➢ Retrospectively identified patients who underwent ▪ Bone scan AND PSMA PET-CT ▪ Within 60 days of each other ➢ Comparison of imaging findings ➢ Additional or discordant findings identified on bone scan: ▪ Review of imaging by both authors ▪ Chart review & review of follow-up imaging, if available	➢ 111 patients identified ➢ Only 7 patients with discordant/additional sites of uptake on bone scan ▪ 1 : Falsely negative PSMA PET and & changed management ▪ 1 : Multiple metastases on both scans; did not change management ▪ 5 : Likely false positive/benign variants; no change in management	✓ Bone scans provide minimal additional benefit when used together with PSMA PET-CT ✓ Simplification of PCa work-up ✓ Cost reduction

Results

- A total of **111 patients**
- Only **seven** (6.3%) patients demonstrated additional or discordant sites of uptake on bone scans
  - **One** patient with false negative on PSMA PET and multiple metastases on bone scan; progressive skeletal metastases on CT follow up (Fig 1)
    - ✓ **Change in management**
  - **Two** patients with false positive bone scans with skull foci due to benign variants
    - ✗ **No change in management**
  - **Two** patients with bone scan positive - PSMA negative rib lesions followed up for 2 and 6 years, remained stable (one is shown in Fig 2)
    - ✗ **Likely benign & No change in management**
  - **One** patient with widespread skeletal metastases on PSMA PET and sites of discordant uptake on bone scan
    - ✗ **No change in management**
  - **One** patient had two additional pelvic sites of uptake on bone scan, followed up for 20 months, likely benign
    - ✗ **No change in management**
  - None of these patients received prior external beam radiation to discordant sites or radionuclide therapy

Implications

- Simplified work-up of Prostate Cancer
- Reduction in expenses
- May lead to a change in response assessment guidelines

Conclusion

- Bone scans provide minimal additional benefit when used in conjunction with PSMA PET-CT imaging in prostate cancer to identify additional sites of disease and effect treatment change
- In pre-treatment planning for Lu^{177}-PSMA therapy, the percentage of PSMA negative disease identified by bone scans is small and of questionable significance

References
1. *J Nucl Med*. 2023;64(11):1744-1747. PMID 37591547
2. *AJR Am J Roentgenol*. 2022;219(3):386-395. PMID 35441529

Evaluating the PRIMARY Score: A Comparative Analysis of PSMA PET and mpMRI for Detecting Clinically Significant Prostate Cancer

Moein Moradpour[1], Lana Al Doori[2], Mona-Elisabeth R Revheim[3], Thomas Werner[1], Abass Alavi[1]

[1]University of Pennsylvania, Department of Radiology, Philadelphia, PA; [2]Drexel University College of Medicine, [3]Oslo University Hospital and University of Oslo

Purpose

- Multiparametric MRI (mpMRI) is the current standard for imaging in prostate cancer diagnosis but has limitations in negative or indeterminate cases, often leading to unnecessary biopsies.
- The 68Ga-PSMA-11 PET/CT-based PRIMARY score is a novel imaging tool that may offer enhanced diagnostic performance for clinically significant prostate cancer (csPCa).
- This study reviews the diagnostic value of the PRIMARY score, comparing it with mpMRI and evaluating its potential role in combined imaging strategies.

Methods

- Systematic literature review conducted using PubMed and Google Scholar
- Search terms included: *"PSMA PET," "Prostate Cancer," "PRIMARY score"*
- Extracted data on sensitivity, specificity, PPV, and NPV for PRIMARY score and mpMRI in detecting csPCa

Results

Figure 1. Five-point PRIMARY score.

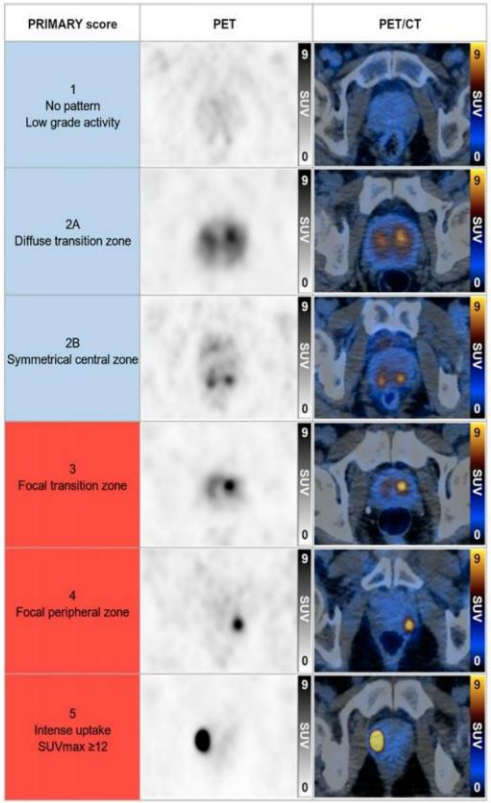

Diagnostic Performance of PRIMARY Score, mpMRI, and Combined Imaging in a 227-Patient Study

Modality	Sensitivity	Specificity	PPV	NPV
PRIMARY Score	86%	76%	88%	72%
mpMRI (PI-RADS)	89%	74%	88%	76%
Combined Imaging	94%	68%	86%	85%

Table 1: This table compares the diagnostic accuracy of PSMA PET using the PRIMARY score, mpMRI (PI-RADS), and a combination of both modalities in detecting clinically significant prostate cancer (csPCa). Combined imaging showed the highest sensitivity (94%) and negative predictive value (85%), suggesting improved performance when both techniques are used together.

PRIMARY Score vs. PI-RADS in a Multicenter Study of 291 Men

Modality	Sensitivity	Specificity	PPV	NPV
PRIMARY Score (1–2 vs. 3–5)	88%	64%	76%	81%
PI-RADS (Score 2 vs. 3–5)	83%	53%	69%	72%

Table 2. This figure illustrates the sensitivity, specificity, positive predictive value (PPV), and negative predictive value (NPV) of the PRIMARY score and PI-RADS in a multicenter cohort. The PRIMARY score outperformed PI-RADS in all categories, particularly in NPV (81% vs. 72%) and specificity (64% vs. 53%), indicating better ability to rule out csPCa.

Comparison of PRIMARY Score and PI-RADS in a 431-Patient Study

Modality	Sensitivity	Specificity	PPV	NPV
PRIMARY Score	90.6%	61.1%	71.4%	85.8%
PI-RADS	87.9%	49.0%	64.9%	79.1%

Table 3. This table presents performance metrics of the PRIMARY score and PI-RADS in a large patient cohort. The PRIMARY score showed higher sensitivity (90.6% vs. 87.9%), specificity (61.1% vs. 49.0%), PPV (71.4% vs. 64.9%), and NPV (85.8% vs. 79.1%), demonstrating superior diagnostic accuracy for detecting clinically significant prostate cancer.

Conclusion

- The PRIMARY score demonstrates strong diagnostic accuracy, with sensitivity and predictive performance comparable to—and in some cases better than—mpMRI.
- Combined use of PRIMARY and mpMRI improves diagnostic precision and may reduce unnecessary biopsies, particularly in patients with equivocal MRI findings.
- The PRIMARY score is a promising adjunct tool in prostate cancer imaging and may be applicable beyond 68Ga tracers with further research.
- Further studies are warranted to validate the PRIMARY score's performance with other PSMA PET tracers (e.g., 18F-labeled agents) and in broader clinical contexts.

References

1. Emmett L, Papa N, Counter W, et. al. Reproducibility and Accuracy of the PRIMARY Score on PSMA PET and of PI-RADS on Multiparametric MRI for Prostate Cancer Diagnosis Within a Real-World Database. J Nucl Med. 2024 Jan 2;65(1):94-99. doi: 10.2967/jnumed.123.266164. PMID: 38050155.

#251888: Impact of ^{68}Ga-PSMA-11 PET/CT on Clinical Management of Prostate Cancer Patients in Different Clinical Settings

Alireza Ghodsi, Avanti Gulhane, Ridvan Demirci, Jonathan Shuhendler, Roman Gulati, Atreya Dash, William Ellis, Yaw Nyame, George Schade, Jonathan Wright, Smith Apisarnthanarax, Jonathan Chen, Jay Liao, Kent Wallner, Heather Cheng, Petros Grivas, Andrew Hsieh, John Lee, Bruce Montgomery, Peter Nelson, Michael T. Schweizer, Todd Yezefski, John Wu, Rafee Talukder, Evan Y. Yu, Daniel W. Lin, Amir Iravani, ***Delphine L. Chen***

2025 SNMMI Poster Award Candidate

Background

- Gallium-68 prostate-specific membrane antigen-11 positron emission tomography/computed tomography (^{68}Ga-PSMA-11 PET/CT) outperforms conventional imaging for detecting prostate cancer (PCa).
- There is limited data descriging how this advanced imaging influences clinical decisions in real-world clinical settings.

Purpose

- Investigating the impact of ^{68}Ga-PSMA-11 PET/CT on management at initial staging (IS), biochemical recurrence (BCR), and at either time point among patients with equivocal lesions on conventional imaging (EL).
- Examining the associations between scan positivity and PSMA-expressing total tumor volume (TTV) with baseline characteristics

Methods

- Patients with pathology-proven PCa were recruited into three cohorts:
  1. **IS** prior to planned definitive therapy for patients with Grade Group ≥4 disease or PSA >20.
  2. **BCR** (as defined by AUA or ASTRO) after surgery or radiation.
  3. **EL** based on conventional imaging obtained for IS (any grade disease) or BCR (any rise in PSA).
- Initial management plans were documented before ^{68}Ga-PSMA-11 PET/CT, and changes in management were tracked for up to 6 months after the scan and categorized as:
  - **Major:** change in treatment modality
  - **Minor:** modification within the same modality
- Multivariate models evaluated associations between scan positivity and TTV with clinical parameters, including age, Gleason score, PSA, and PSA doubling time (PSADT).
- IS and BCR cohorts included EL patients for multivariate analyses.

Results

101 men with a median age of 68 years (IQR: 64-74) were enrolled:

Characteristic		IS (N=29)	BCR (N=30)	EL (N=42)
Age		67 (62, 70)	71 (65, 75)	68 (65, 74)
PSA		16 (8, 31)	1 (1, 4)	9 (5,20)
WHO grade group		4 (3,5)	3 (2, 5)	3 (2, 5)
Gleason score	≤ 6	0 (0)	2 (6.7)	1 (2.4)
	7	10 (34)	17 (57)	21 (50)
	≥ 8	19 (66)	11 (37)	20 (48)

^{68}Ga-PSMA-11 PET/CT positivity was marginally significantly associated with Gleason score (OR:4.3; 95%CI 1.2-27.6; p=0.057) after adjusting for age and PSA level in the BCR cohort.

^{68}Ga-PSMA-11 PET/CT detection rates:

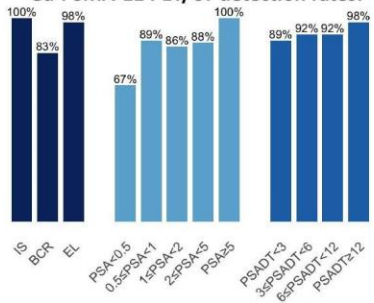

Changes in clinical management following ^{68}Ga-PSMA-11 PET/CT:

- **IS:** Management changed in **31%** of patients (8 major, 1 minor)
- **BCR:** Management changed in **60%** of patients (15 major, 3 minor)
- **EL:** Management changed in **62%** of patients (23 major, 3 minor)

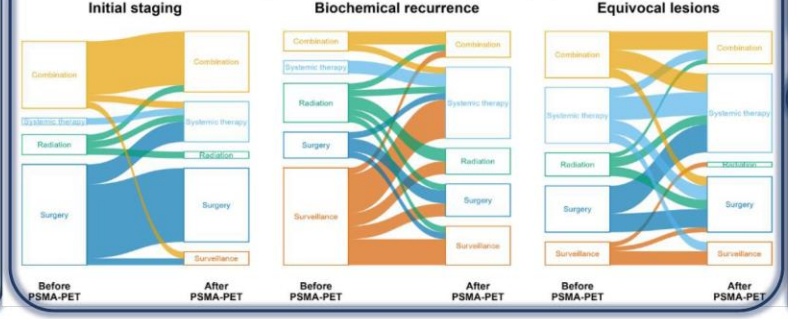

PSA was weakly associated with TTV after adjusting for age and Gleason score in the IS cohort (doubling PSA was associated with 1.3-fold increase in TTV; p=0.07) and strongly associated in the BCR cohort (1.6-fold increase; **p<0.001**) and EL cohort (1.5-fold increase; **p<0.001**).

Age and Gleason score were independently associated with TTV only in the **BCR cohort**.

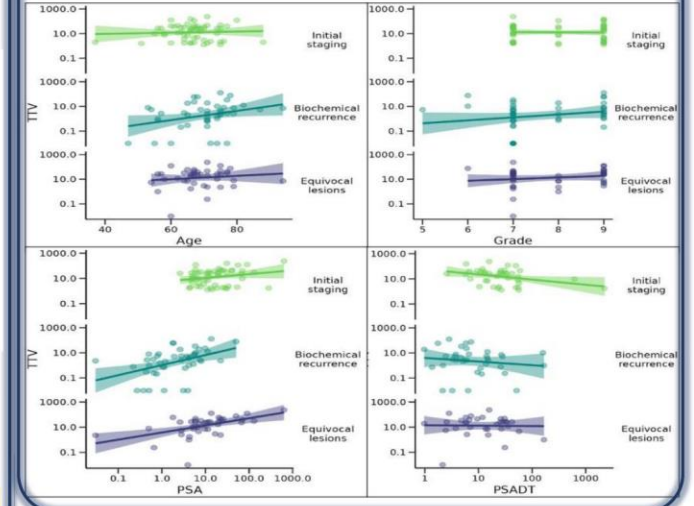

Conclusion

- ^{68}Ga-PSMA-11 PET/CT is a promising diagnostic method for patients with PCa in clinical practice, achieving a **94%** overall detection rate.
- It impacted clinical management in **58%** of cases, especially in patients with **BCR or equivocal lesions**.

Knowledge-based semantic enrichment of medical imaging data for automatic phenotyping and pattern discovery in metastatic lung cancer

Francesco Cremonesi[1], Lucie Chambon[1], Nelson Mokaddem[2], Huyen Trang Nguyen[1], Olivier Humbert[2,3], Marco Lorenzi[1]
[1] Inria Center at Université Côte d'Azur, Epione Research Group, France
[2] Department of Nuclear Medicine, Centre Antoine Lacassagne, Université Côte d'Azur (UCA), 33 Avenue de Valombrose, 06189 Nice, France
[3] Université Côte d'Azur, CNRS, Inserm, iBV, Nice, France

1. INTRODUCTION

A) CONTEXT

The emergence of AI models for the segmentation of 18-FDG PET/CT images has opened the way for **automatic quantification of clinically-relevant parameters in metastatic cancer patients**. However, current approaches **lack specificity** as they do not provide information about the localisation of lesions, which is a major clinical parameter for patient management. These methods also **lack generality**, as they fail to integrate the medical community's body of anatomical knowledge, which can nowadays be found in machine-readable ontology formats.

B) OBJECTIVES

Semantic enrichment of lesion annotations through the automatic segmentation of anatomical structures and inclusion of ontological knowledge. Demonstrate how such integration improves analysis depth, interpretability, as well as reusability of the data for secondary purposes, by enabling reasoning at different anatomical scales and linking with other sources of information such as clinical records.

C) DATA

Whole-body 18-FDG PET/CT scans from a cohort of **metastatic non-small cell lung cancer (NSCLC) patients undergoing immunotherapy treatment** (*n=101*) from Centre Antoine Lacassagne were included. The dataset included:
i) **automatic organ segmentations on CT** using TotalSegmentator [1]
ii) **manual lesion segmentations on FDG PET** by doctors
iii) **Manual annotation of lesion location** ,at the organ level, by doctors, termed « **reference organ labels of lesions** »

[1] Wasserthal, Jakob, et al. "TotalSegmentator: robust segmentation of 104 anatomic structures in CT images." *Radiology: Artificial Intelligence* 5.5 (2023): e230024.
[2] Rosse, Cornelius, and José LV Mejino Jr. "A reference ontology for biomedical informatics: the Foundational Model of Anatomy." Journal of biomedical informatics 36.6 (2003): 478-500.

2. METHODS

A) MAPPING IMAGING STRUCTURES TO ANATOMICAL KNOWLEDGE

We mapped the roughly 100 TotalSegmentator structures and the human-defined gold-standard labels to the Foundational Model of Anatomy (FMA) ontology [2] using a mix of automatic heuristics and human post-hoc oversight. Each structure was then associated with **reference organ labels of lesions** by querying the ontology using the SparQL language for hierarchical or inclusion relationships such as *subClassOf*, *member_of*, and others. A small number of associations between one anatomical structure and multiple gold-standard labels were refined using simple prioritization heuristics.

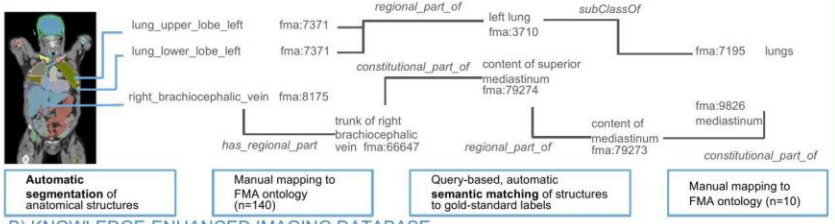

B) KNOWLEDGE-ENHANCED IMAGING DATABASE

We computed the intersection between the manual lesion segmentations on PET performed by doctors and the automatic organ segmentations on CT, generated by TotalSegmentator, and combined intersections belonging to the same class as defined by the **reference organ labels of lesions**. We localised lesions by finding classes with the maximal intersection.

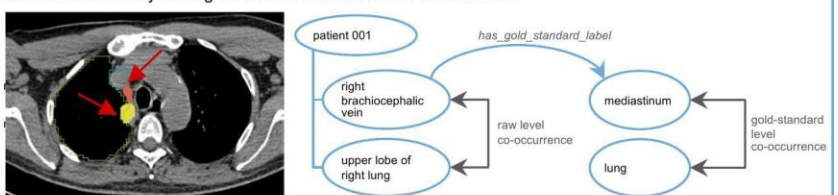

A Knowledge Graph (KG) integrating the FMA ontology allows the extraction of the co-occurrence of lesions at two semantic scales: the raw TotalSegmentator structures and the **reference organ labels**. In both cases, we perform KMeans clustering to stratify patients based on patterns of lesion co-occurrence.

3. RESULTS

Ontology-based mapping of anatomical structures enabled automatic validation of the lesion localization algorithm. The simple intersection-based algorithm **successfully localized 1572 out of 1962 lesions (80.1 %)** across all lesion sizes.

Patient phenotyping based on the knowledge-enhanced organ labels allowed for **more interpretable clusters** that could be used for **better correlation with survival metrics** and more precise quantitative imaging

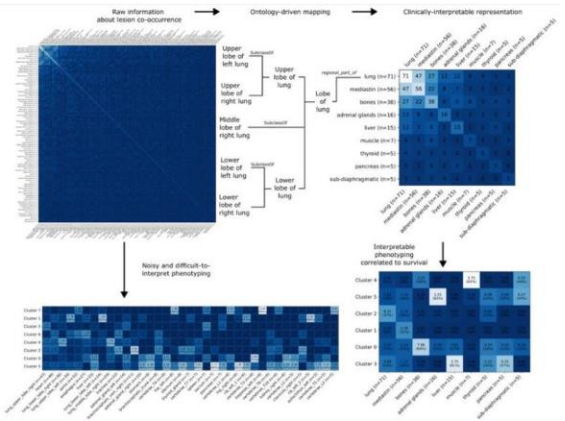

4. CONCLUSION

Automatic segmentation of anatomical structures on paired CT scans can enriched 18-FDG PET lesion annotations, with the aim to **integrate anatomical knowledge into imaging data**.

Analysis of these enriched PET imaging data yielded **better clinical interpretability** when compared to the raw data and could be used to improve **correlation between PET imaging and outcome in cancer patients.**

MetaPredictomics: A Comprehensive Approach to Predict Post-Surgical NSCLC Recurrence Using Clinicopathological, Radiomics, and Organomics Data

Mehdi Amini[1], Ghasem Hajianfar[1], Yazdan Salimi[1], Zahra Mansouri[1], and Habib Zaidi[1†]

[1]Division of Nuclear Medicine and Molecular Imaging, Geneva University Hospital, Geneva, Switzerland

This work was supported by the Swiss National Science Foundation with grant SNRF 320030_231742

INTRODUCTION

- Recurrence is the primary cause of treatment failure in Non-Small Cell Lung Cancer (NSCLC), significantly reducing both survival rates and quality of life.
- NSCLC is a complex disease characterized by diverse clinical, genetic, and histopathological traits.
- This necessitate personalized treatment approaches.
- Numerous biomarkers have been introduced for NSCLC prognostication; however, no single source of information can provide a comprehensive understanding of the disease.
- Integrating biomarkers from multiple sources may offer a holistic view of the disease, enabling more accurate predictions.
- In this study, we present MetaPredictomics, a framework that integrates clinicopathological data with PET/CT radiomics from the primary tumor and presumed healthy organs to predict post-surgical recurrence.

METHODS

- Dataset: 145 NSCLC patients sourced from an online dataset.
- Segmentation: A fully automated deep learning model to delineate 19 organs on the CT compartment of the pre-surgical PET/CT scans.
- Radiomics: Using PyRadiomics, 214 features (107 from CT, 107 from PET) were extracted from the gross tumor volume (GTV) and each segmented organ.
- Clinical feature set: based on clinicopathological, gene mutation status, and treatment history.

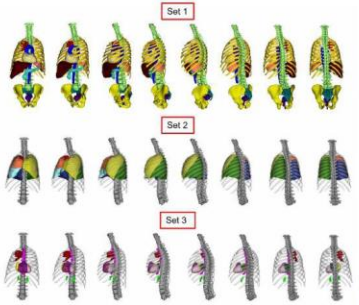

Figure 1. An example of the organs segmented on the CT image of a patient in 3D visualization.

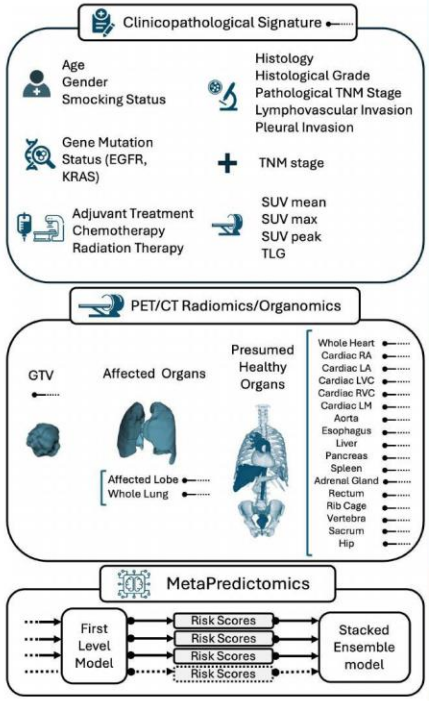

Figure 2. The proposed MetaPredictomics framework for predicting NSCLC recurrence.

- First level model: a time-to-event prediction machine, based on Glmboost.
- Meta Model: The hazard ratios obtained from the first level models were then used as inputs for meta models developed using a stacked ensemble approach.
- Questing optimized performance, we assessed meta models established upon all possible combinations of first level models with C-index≥0.6.
- Evaluation: The performance of all the models was evaluated using the average concordance index (C-index) across a unique 3-fold cross validation scheme for fair comparison.

RESULTS

- The Clinicopathological model outperformed other first level models with C-index of 0.67.
- GTV radiomics model achieved C-index of 0.65.
- Among the organomics models, whole-lung and aorta models achieved top performance with C-index of 0.65.
- In total 12 organomics models achieved C-indices of ≥ 0.6.

Table 1. The results of the first-level models for each test fold as well as the average value of the three test folds in concordance index (C-index).

Model	Fold 1	Fold 2	Fold3	Average
Clinicopathological	0.74	0.69	0.57	0.67
GTV	0.71	0.62	0.61	0.65
Affected Lung Lobe	0.66	0.63	0.59	0.63
Whole Lung	0.72	0.63	0.61	0.65
Whole Heart	0.61	0.6	0.6	0.6
Cardiac Right Artrium	0.58	0.56	0.59	0.58
Cardiac Left Artium	0.58	0.55	0.6	0.58
Cardiac Left Ventricle Cavity	0.65	0.57	0.59	0.61
Cardiac Right Ventricle Cavity	0.6	0.6	0.6	0.6
Cardiac Left Myocardium	0.59	0.57	0.61	0.59
Aorta	0.67	0.58	0.68	0.65
Esophagus	0.62	0.65	0.63	0.63
Liver	0.67	0.58	0.59	0.62
Pancreas	0.58	0.62	0.62	0.61
Spleen	0.59	0.61	0.59	0.6
Adrenal Glands	0.62	0.57	0.69	0.63
Rectum	0.57	0.56	0.6	0.58
Rib Cage	0.61	0.56	0.6	0.59
Vertebra	0.58	0.56	0.62	0.59
Sacrum	0.62	0.6	0.62	0.62
Hip	0.56	0.57	0.59	0.58

- Meta models significantly outperformed the first level models with the top 100 achieving C-indices between 0.703 to 0.731.
- The clinicopathological, whole lung, esophagus, pancreas, and GTV models were the most frequently present models in the top 100 meta models with frequencies of 98, 71, 69, 62, 61, respectively.

Table 2. The performance of the top 10 meta-models sorted by their average C-index over the three test folds. Result of each fold is as well presented.

	Models	Fold 1	Fold 2	Fold 3	Average
1	Clinical+GTV+Whole Lung+Esophagus+Pancreas	0.800	0.685	0.709	0.731
2	Clinical+GTV+Whole Lung+Sacrum	0.816	0.639	0.738	0.731
3	Clinical+GTV+Whole Lung+Pancreas+Sacrum	0.816	0.641	0.731	0.730
4	Clinical+Affected Lung Lobe+Whole Lung+Esophagus+Pancreas	0.766	0.725	0.696	0.729
5	Clinical+Whole Lung+Esophagus	0.783	0.733	0.670	0.729

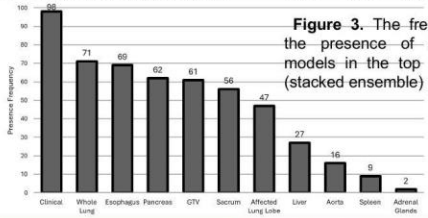

Figure 3. The frequency of the presence of first level models in the top 100 meta (stacked ensemble) models.

CONCLUSION

In this study we highlighted the value of maximizing the use of medical imaging for NSCLC recurrence prognostication by incorporating data from various organs, rather than focusing solely on the tumor and its immediate surroundings.

This multi-source integration proved particularly beneficial in the meta models, where combining clinicopathological data with tumor radiomics and organomics models significantly enhanced recurrence prediction.

Assessment of PET Drug Adverse Events over the Last Half Century

Marianna Dakanali[1,2], Peter J. H. Scott[1,2], Henry F. VanBrocklin[2,3], Steven S. Zigler[2,4]

[1] Department of Radiology, University of Michigan, Ann Arbor, MI
[2] Coalition of PET Drug Manufacturers, Fredericksburg, TX
[3] Department of Radiology and Biomedical Imaging, University of California San Francisco, San Francisco, CA
[4] Siemens PETNET Solutions, Knoxville, TN

MICHIGAN MEDICINE
UNIVERSITY OF MICHIGAN

COALITION OF PET DRUG MANUFACTURERS

2025 SNMMI Poster Award Candidate
SNMMI Annual Meeting
ACCELERATING THE CURE

Introduction

Multiple new PET Radiopharmaceuticals (RPhs) have recently been approved by the US Food and Drug Administration (FDA). Despite the generally accepted safety profile of PET RPhs over millions of studies per year, the microdoses used in most studies, and low incidence of adverse events (AEs),[1-4] there appear to be elevated concerns from regulatory authorities regarding the safety of PET RPhs in recent years. The FDA Adverse Events Reporting System (FAERS) Public Dashboard was established in 1969 and is an open access database which collects AEs or other pharmaceutical errors reported by patients, providers or the drug manufacturers.[5] This retrospective study assesses risks associated with PET RPhs by reviewing AEs reported through FAERS since 21 CFR 212 was implemented in 2012.

Methods

Data for AEs reported to FDA for approved PET RPhs were collected using FAERS during December 2024 for global AEs reported between 2012 and September 30th, 2024. FDA approved PET radiopharmaceuticals were searched using all known names for each drug, both generic and brand names. The following tables were downloaded from the database: a. case count by received year; b. cases by reaction; and c. listing of cases. AE reports were categorized as depicted in **Figure 1**.

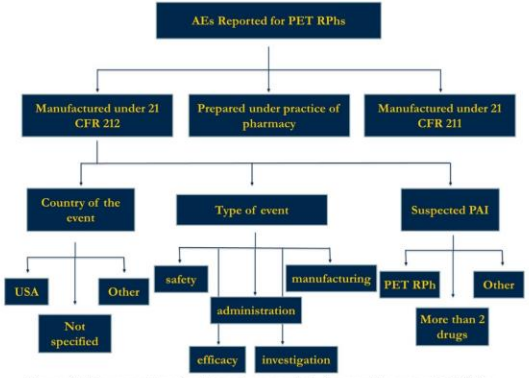

Figure 1. AEs were categorized based on manufacturing regulatory oversight. RPhs manufactured under 21 CFR 212 were further analyzed based on country of the event, type of the event and suspected Product Active Ingredient (PAI)

Results

Collectively, more than 23.2 million AE reports for all drug products were transmitted to FDA between January 2012 and September 2024. The total number of reports submitted for all FDA-approved PET RPhs was 1,011. Of those, 7 cases were removed as duplicates bringing the total number of reports to 1,004, representing only 0.0043% of AEs reported to the FDA for the specified time period. Of these 1,004 cases, 508 (0.0022%) were associated with PET drugs manufactured under 21 CFR part 212, and 353 (0.0015%) were related to drugs prepared in pharmacies or nuclear medicine departments under the practice of pharmacy or medicine. The remaining 143 reports (0.0006%) were filed for rubidium-82 (Rb-82) generators manufactured under 21 CFR part 211 (**Figure 2**).

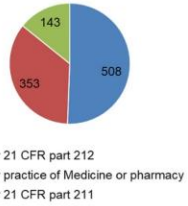

Figure 2: Number of reported AEs associated with PET radiopharmaceuticals manufactured in facilities under 21 CFR part 212 (blue), using kits in pharmacies or nuclear medicine departments under practice of pharmacy or medicine (red), or Rb-82 generators manufactured under 21 CFR part 211 (green).

Reported AEs Based on Country Event Occurred

Of the 1,004 total cases, 810 (81%) occurred in the US, 133 (13%) in other countries, while the country for the remaining 61 cases (6%) was not specified (**Figure 3A**). For the 508 AEs associated with PET RPhs manufactured under the cGMP requirements in 21 CFR 212, only 353 of the reported AEs occurred in the United States (**Figure 3B**).

Reported AEs Based on Type of Event Reported

The 508 reported cases for PET RPhs manufactured according to 21 CFR 212 were classified based on the type of event reported. Events were categorized as related to safety or efficacy of the drug, drug administration errors, manufacturing problems, and events reported as either a false positive or false negative investigation. The results are depicted in **Figure 4** and detailed in **Table 1**.

Results

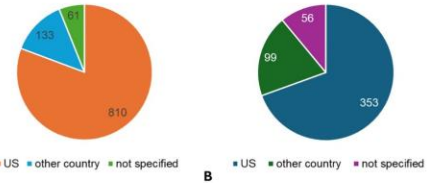

Figure 3: **A**. Number of reports for PET RPhs based on the country where the event occurred. **B.** Number of reports for PET RPhs manufactured under 21 CFR part 212 based on the country where the event occurred.

Table 1: Adverse Events Categorized by Type and Radiopharmaceutical

Drug	Safety	Efficacy	Administration	Investigation	Manufacturing
Ammonia N-13	2	0	0	0	0
Fluciclovine F-18	14	34	15	11	2
Fluoroestradiol F-18	1	1	0	4	0
Florbetaben F-18	6	0	0	0	0
Florbetapir F-18	55	2	6	0	1
Flutemetamol F-18	81	5	1	0	0
Sodium Fluoride F-18	1	1	0	0	0
Flotufolastat F-18	1	9	0	1	0
Piflufolastat F-18	24	60	9	3	19
Fludeoxyglucose F-18	115	7	6	1	10
Total	**300**	**119**	**37**	**20**	**32**

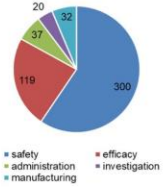

Figure 4: Number of reports for PET RPhs manufactured in cyclotron facilities based on the type of the AE.

Reported AEs Based on Suspected Product Active Ingredient (PAI)

Finally, the suspected Product Active Ingredient (PAI) was reviewed and separated into three categories: a) the PET drug PAI, b) a different drug PAI or c) more than two PAIs reported. As shown in **Figure 5**, for 22 cases a different drug was suspected of causing the adverse event, and for 85 cases at least one more drug besides the PET radiopharmaceutical was suspected.

Results

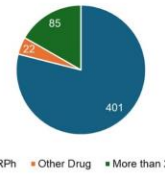

Figure 5: Number of reports for PET RPhs based on the suspected Product Active Ingredient.

Combining all the different parameters used for our analysis, we found that for the past 12 years there were only 349 cases transmitted to the FAERS for PET radiopharmaceuticals manufactured in the US and unspecified countries under 21 CFR part 212 that caused an adverse event for which the PET drug was the suspected product active ingredient. Of those 349 cases only 152 were regarding an adverse drug reaction and thus concerned the safety profile of the PET drugs. Additionally, the number of AEs in the US for PET drug as the suspected PAI and related to manufacturing or sterility problems were 48.

Conclusions

Despite the increased concerns regarding the safety of PET RPhs from regulators in recent years, our analysis of the AEs reported to the FAERS public dashboard revealed that the number of AEs remains extremely low (less than 81 AEs per 10^6 scans per year) compared to the annual number of doses administered (estimated at about 3,000,000).[6] These findings confirm our assertion that PET radiopharmaceuticals can be generally recognized as a safe and effective drug class, for which very low levels of adverse events are observed year to year. It is challenging to conclusively connect reported AEs to PET RPh sterility or production failures and thus, in our opinion this should not be used to justify any revision of regulations.

References

[1] Silberstein, EB. J Nucl Med. 1998; 39:2190-2192.
[2] Silberstein, EB. J Nucl Med. 2014; 55:1308-1310.
[3] Silindir-Guney, M.; Ozolmez, N. J Radioanal Nucl Chem. 2024; Oct 5:1-13
[4] Schreuder, N.; Koopman, D.; et al. Semin Nucl Med. 2019; 49(5):382–410.
[5] https://www.fda.gov/drugs/fdas-adverse-event-reporting-system-faers/fda-adverse-event-reporting-system-faers-public-dashboard
[6] IMV 2024 PET Imaging Market Summary Report, 2024

Prediction of blood-brain barrier penetration of PET CNS drugs enabled by explainable machine learning

Clemens p Spielvogel, Natalie Schindler, Christian Schröder, Sarah Stellnberger, Wolfgang Wadsak, Markus Mitterhauser, Laszlo Papp, Marcus Hacker, Verena Pichler and Chrysoula Vraka, Journal of Nuclear Medicine June 2025, 66 (supplement 1) 251263;

Introduction: The blood-brain barrier (BBB) is a selective barrier that limits the transport of molecules from the bloodstream into the brain. For drugs unfolding their effects in the brain, the inability to cross the BBB can render an otherwise potent drug entirely ineffective. Hence, predicting the penetration of the BBB is crucial for the development of central nervous system (CNS) drugs and is one of the main hurdles for successful clinical phase I studies. In this study, we employ physico-chemical properties derived using experimental measurements and in silico methods to establish a public database and demonstrate that the included parameters can be integrated using machine learning to identify radiolabeled drug candidates capable of penetrating the BBB.

Methods: For a dataset of 154 radiolabeled molecules previously assessed in vivo for BBB penetration, we measured, calculated, and collected a total of 24 molecular parameters including molecular weight, polar surface area (PSA), logP values, hydrogen bond characteristics, and reproducible published scores. We further enhanced these parameters with a novel in silico 3D calculation of non-classical polar surface area. Based on the collected data, we trained and evaluated six machine learning classification models. All models were trained to predict two sets of targets - first, a binary prediction of BBB permeability (yes/no) and second, a multiclass classification differentiating CNS-negative, CNS-positive, and efflux transporters. Validation of the models was performed using a robust stratified 100-fold Monte Carlo (resampling) cross-validation scheme. Explainable artificial intelligence methods such as Shapley additive explanations (SHAP) and surrogate modeling were integrated to interpret the influence of individual molecular parameters on BBB penetration predictions and allow for a simplified visual representation approximating the decision process behind the otherwise opaque models. The resulting machine learning models were further compared with traditional approaches for the prediction of BBB permeability, including the CNS MPO, CNS MPO PET, and the BBB scores.

Results: While multiple individual parameters, including the novel 3D PSA were significantly different ($p<0.05$) in CNS-negative and CNS-positive drugs, none of them were able to reliably predict BBB penetration (AUC<0.57). On the other hand, multiparametric integration via machine learning models outperformed traditional predictive approaches, with a random forest-based classifier achieving the best performance for the binary BBB penetration prediction (AUC 0.88, 95% CI 0.87-0.90) and multiclass efflux transporter versus CNS-positive and CNS-negative prediction (AUC 0.82, 95% CI: 0.81-0.82). SHAP analysis revealed the multifactorial nature of the problem, emphasizing the benefit of multivariate models over single predictive parameters while stressing the importance of the BBB score, the novel 3D PSA, and tPSA. Surrogate modeling demonstrated that the random forest model could be approximated using a simple decision tree model with four and six parameters for binary and multiclass classification respectively. A comparison with existing scoring systems like the CNS MPO (AUC 0.53), CNS MPO PET (AUC 0.51), and BBB (AUC 0.68) scores demonstrated the superior predictive capability of the machine learning model, while also enabling the identification of efflux transporter substrates.

•**Conclusions:** Our integrated machine learning approach utilizing in vivo measurements and novel in silico approaches enables the prediction of BBB penetration, potentially reducing reliance on extensive experimental measurements and animal testing. This study does not only provide the potential to accelerate and reduce costs of CNS drug development for radiopharmaceuticals but also provides the community with a standardized database of radio-labeled molecules and corresponding physico-chemical parameters.